SUPPLEMENTARY MATERIAL

Metal-atovaquone complexes with antiplasmodial activity: chemical reactivity and structure-activity relationships

Luana Daniel,[a] Chris Hebert J Franco,[a, b] Adrielle Sacramento de Morais[c], Arquímedes Karam[a], Marcelo Cecconi Portes,[d] Milena Barros Silva[c], Lisia Maria Gobbo dos Santos,[d] Joel Mosnier,[e,f,g,h] Isabelle Fonta,[e,f,g,h] Ana Maria Da Costa Ferreira,[i] Bruno Pradines,[e,f,g,h] Diogo Rodrigo M. Moreira*[c], Maribel Navarro*[a].

[a] Laboratório de Química Bioinorgânica e Catálise, Departamento Química, Instituto de Ciências Exatas, Universidade Federal de Juiz de Fora, Minas Gerais, Brazil.

[b] MINDlab: Molecular Design & Innovation Laboratory, Instituto Superior Técnico, Universidade de Lisboa, Lisboa, Portugal.

[c] Instituto Gonçalo Moniz, FIOCRUZ. Salvador, Bahia, Brazil.

[d] Instituto Nacional de Controle de Qualidade em Saúde. FIOCRUZ. Rio de Janeiro, Rio de Janeiro, Brazil.

[e] Unité Parasitologie et entomologie, Département risques vectoriels, Institut de recherche biomédicale des armées. Marseille, France.

[f] Aix-Marseille Univ, SSA, AP-HM, RITMES, Marseille, France.

[g] IHU Méditerranée Infection. Marseille, France.

[h] Centre National de Référence du Paludisme. Marseille, France.

[i] Laboratório de Bioinorgânica, Catálise e Farmacologia, Instituto de Química, Universidade de São Paulo, São Paulo, SP, Brazil.

*Corresponding authors: D. R. M. Moreira at diogo.magalhaes@fiocruz.br and M. Navarro at maribel.navarro@ufjf.br.

Table of content

Characterization of metal complexes

Thermogravimetric studies

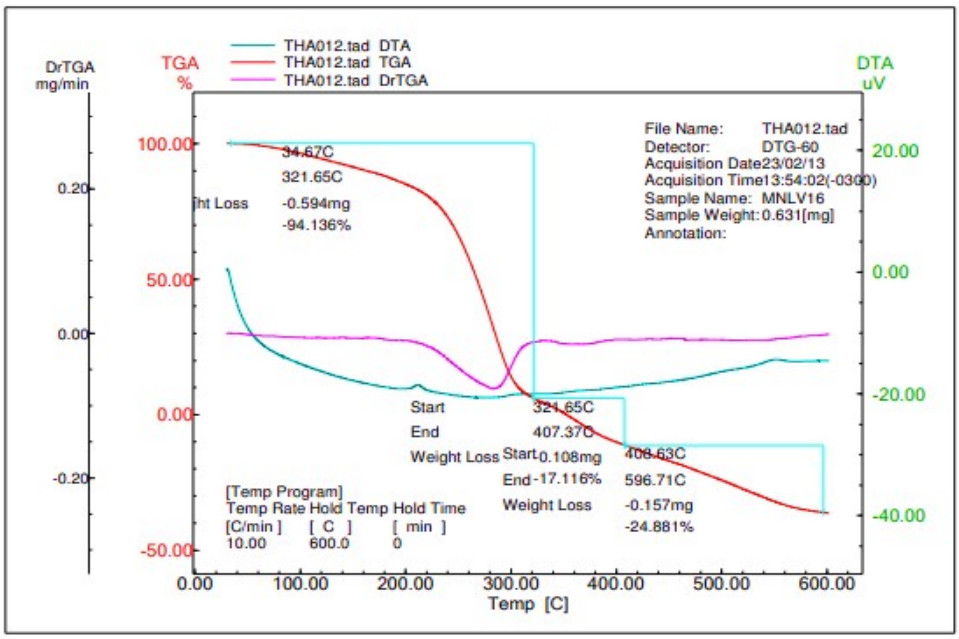

Figure S1: Thermogravimetric curve for the complex [Ag(ATV)]

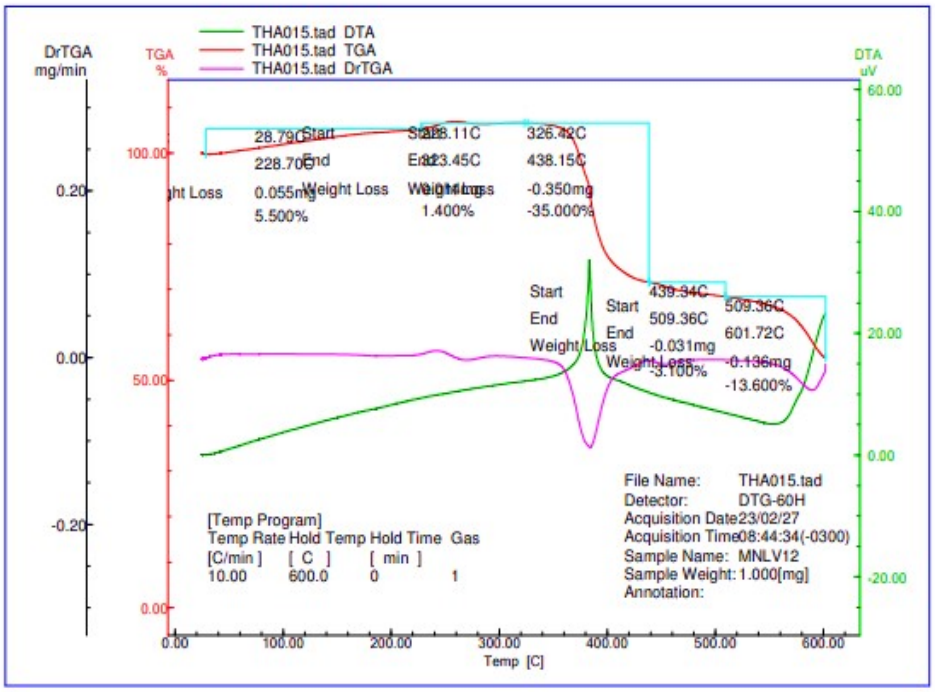

Figure S2: Thermogravimetric curve for the complex $[Zn(ATV)_2(H_2O)_2]\cdot 2H_2O$

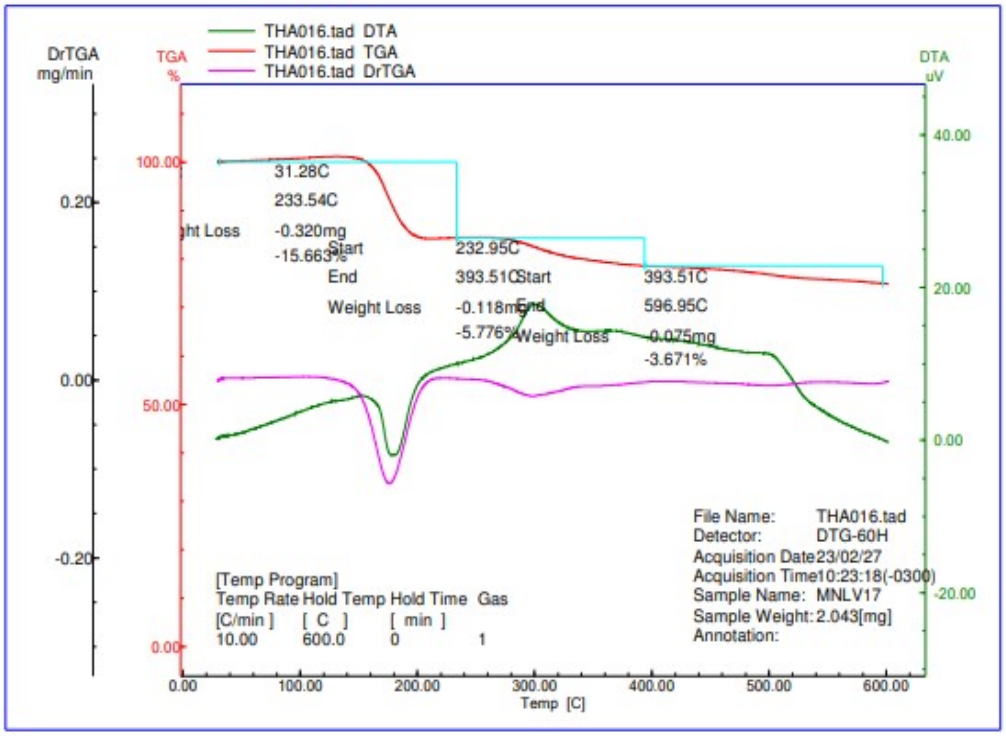

Figure S3: Thermogravimetric curve for the complex $[Zn(ATV)_2(CH_3OH)_2]\cdot H_2O$

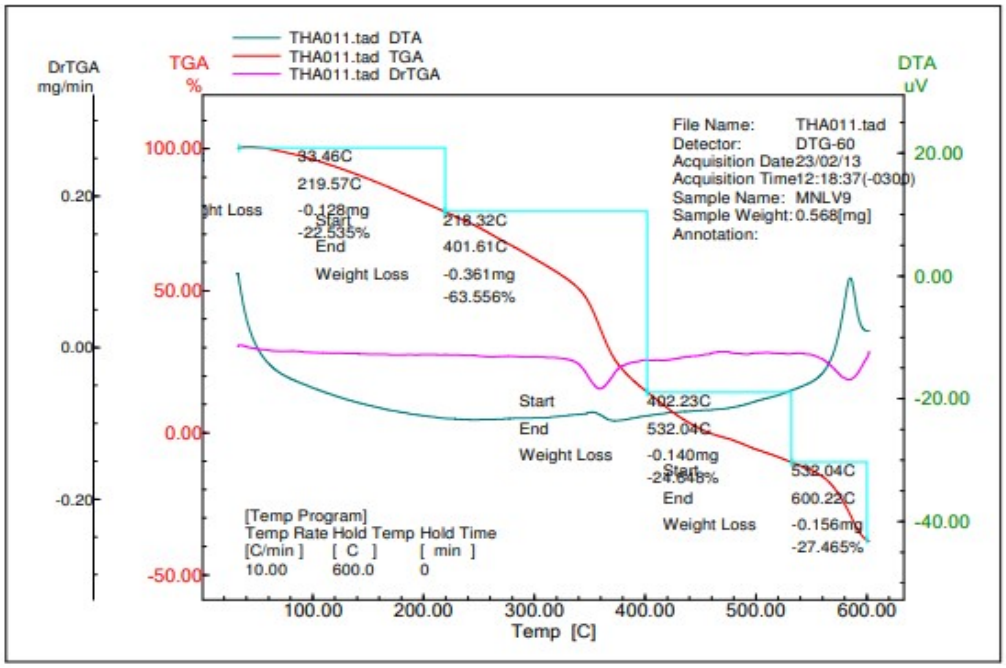

Figure S4: Thermogravimetric curve for the complex $[Zn(ATV)_2]_n$

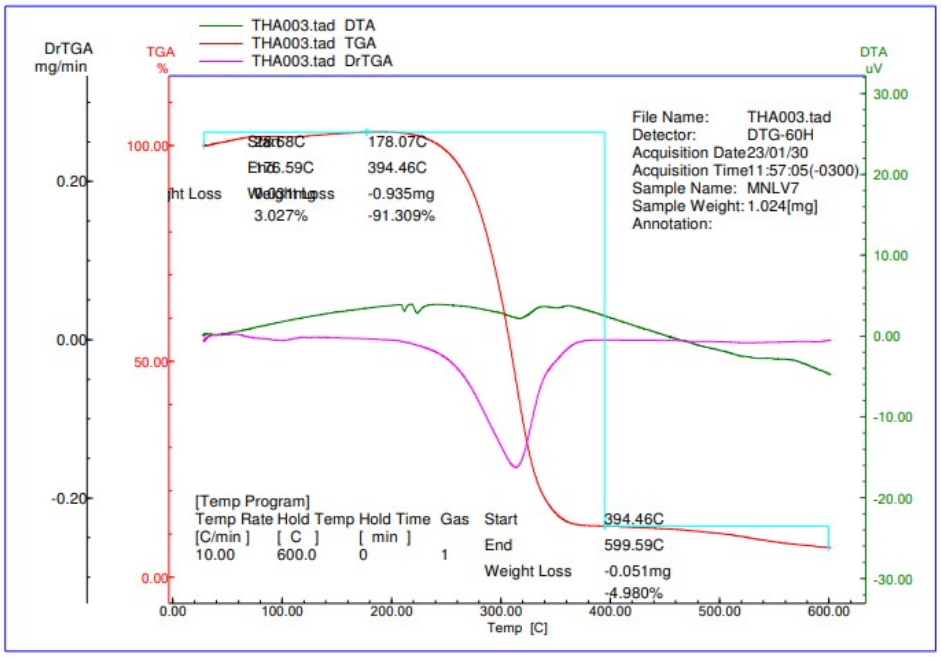

Figure S5: Thermogravimetric curve for the metallic complex [Cu(ATV)$_2$]

Characterization by mass spectrometr.

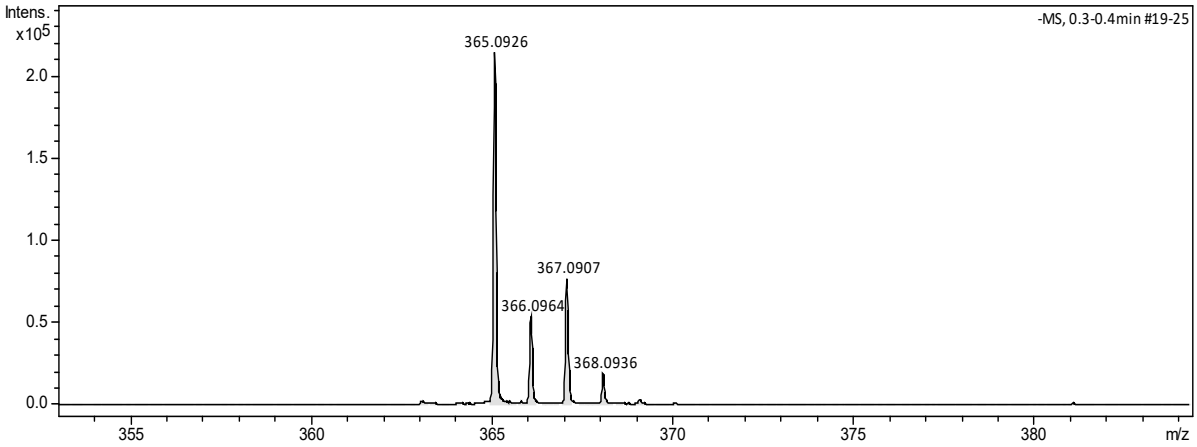

Figure S6: Mass spectrum for Atovaquone

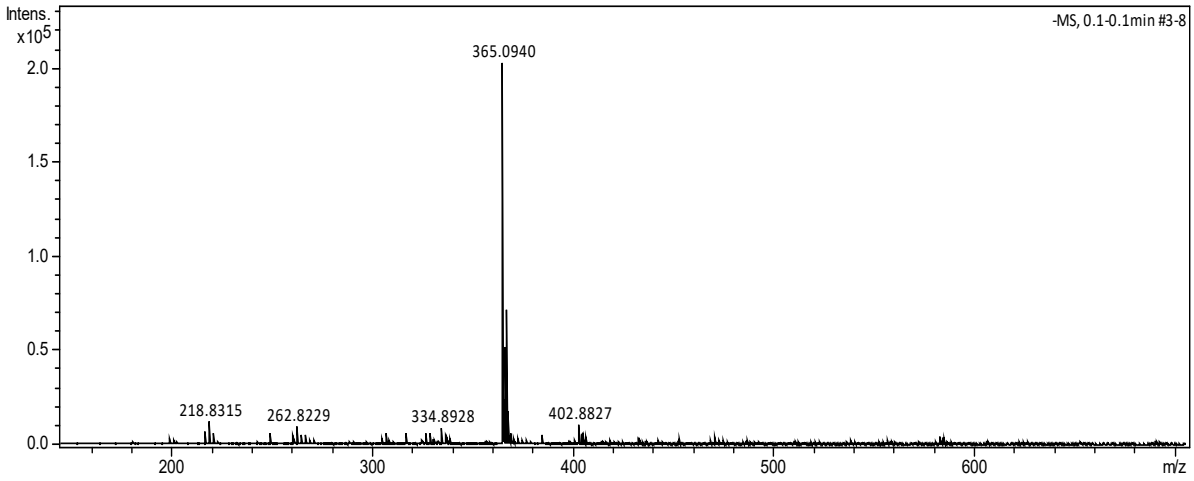

Figure S7: Mass spectrum for [Ag(ATV)] (complex **1**)

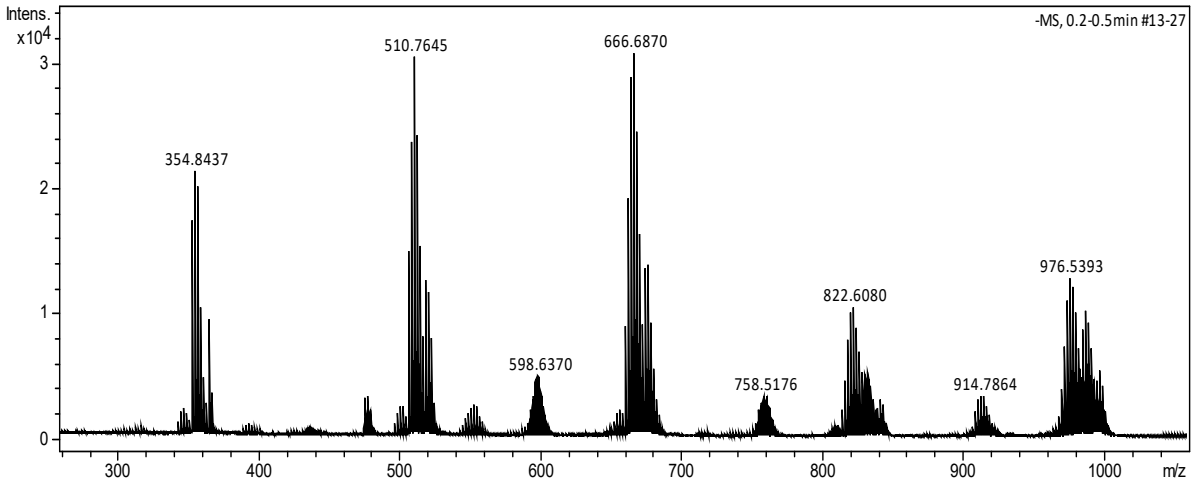

Figure S8: Mass spectrum for $[Zn(ATV)_2(H_2O)_2]\cdot 2H_2O$ (complex **2**)

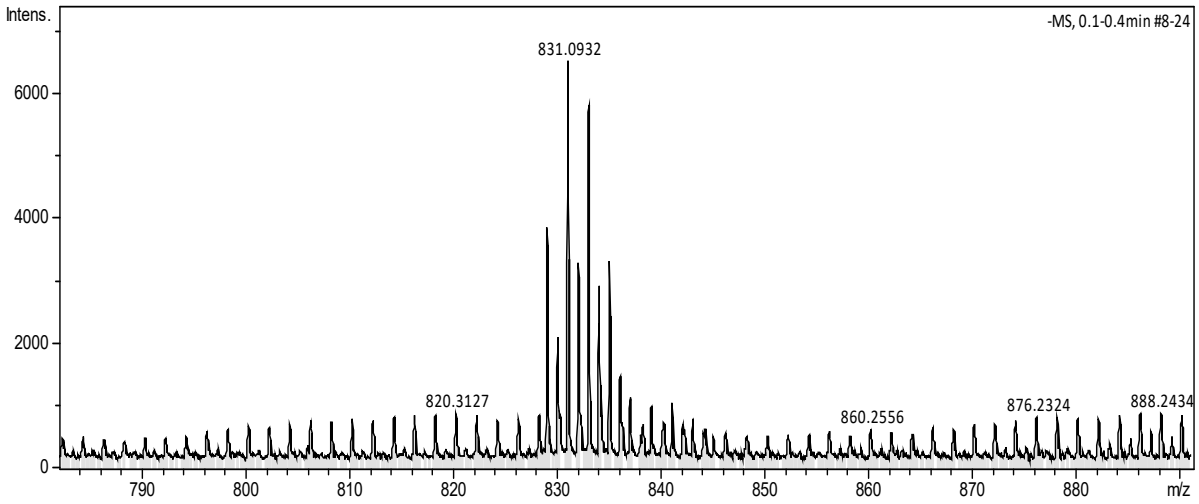

Figure S9: Mass spectra for $[Zn(ATV)_2(CH_3OH)_2]\cdot H_2O$ (complex **3**)

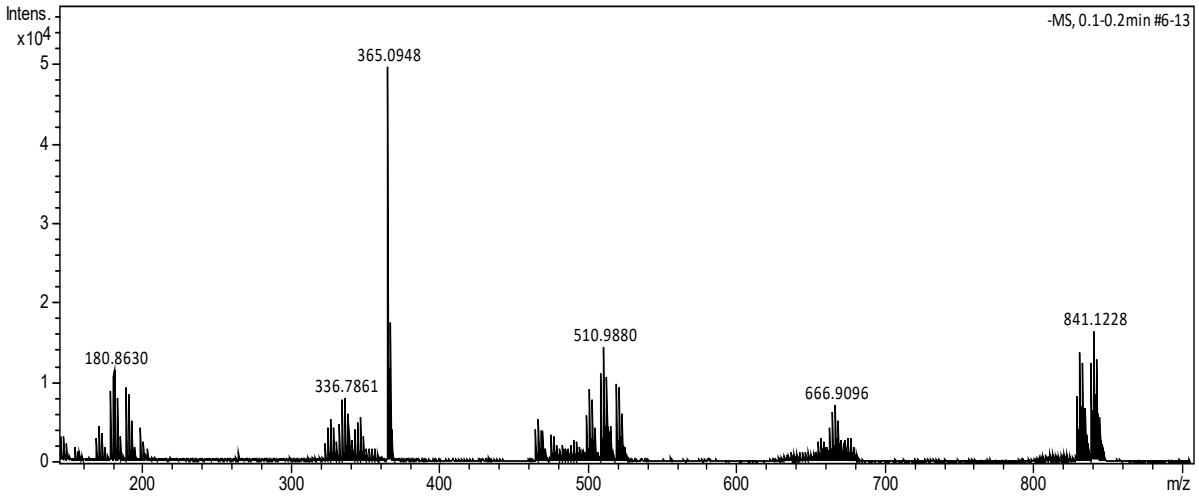

Figure S10: Mass spectrum for $[Zn(ATV)_n]$ (complex **4**)

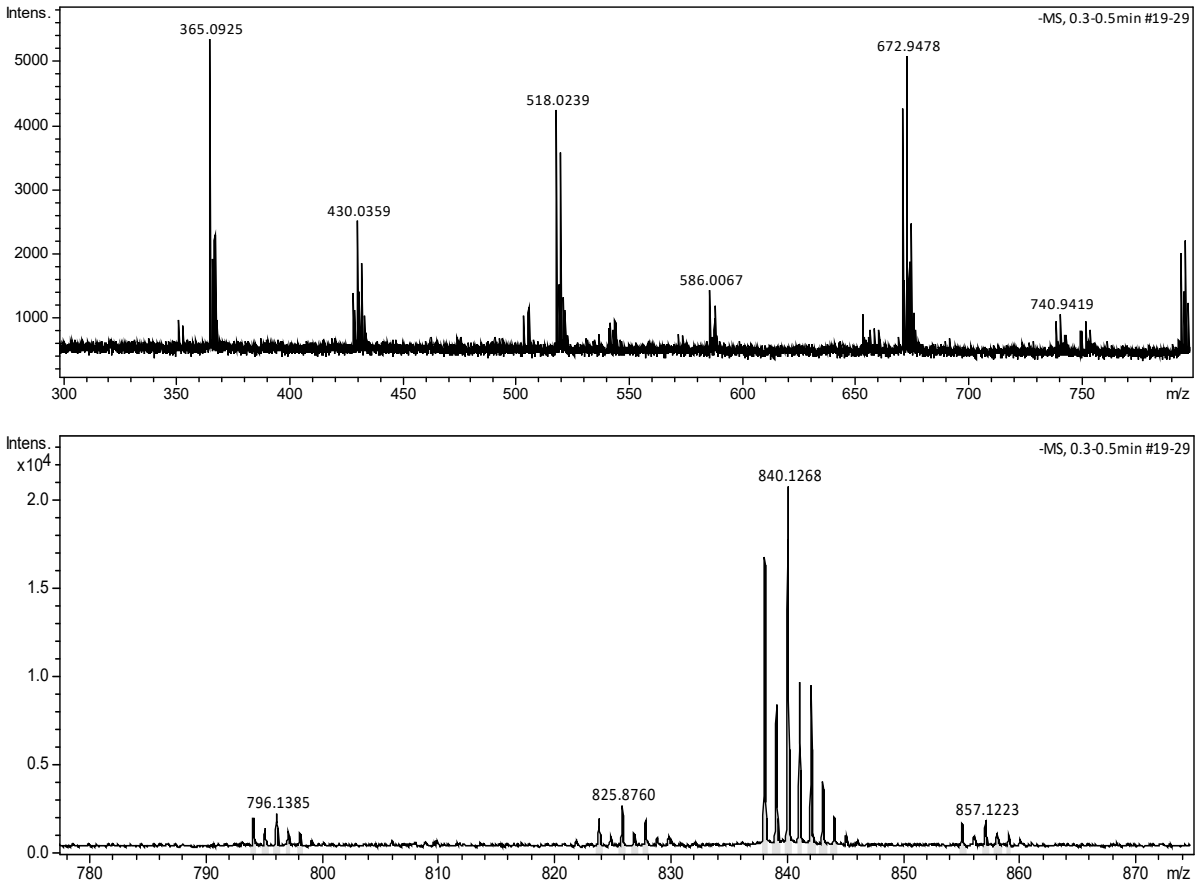

Figure S11: Mass spectra for $[Cu(ATV)_2]$ (complex **5**)

Characterization by UV-Vis spectroscopy

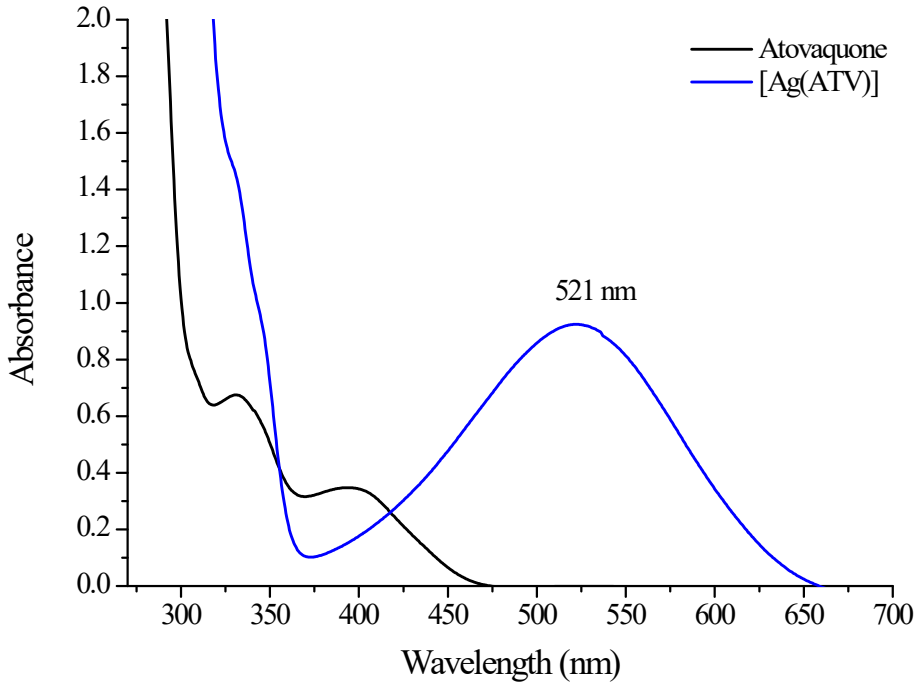

Figure S12: Spectra Uv-Vis of [Ag(ATV)] and ATV in DMSO

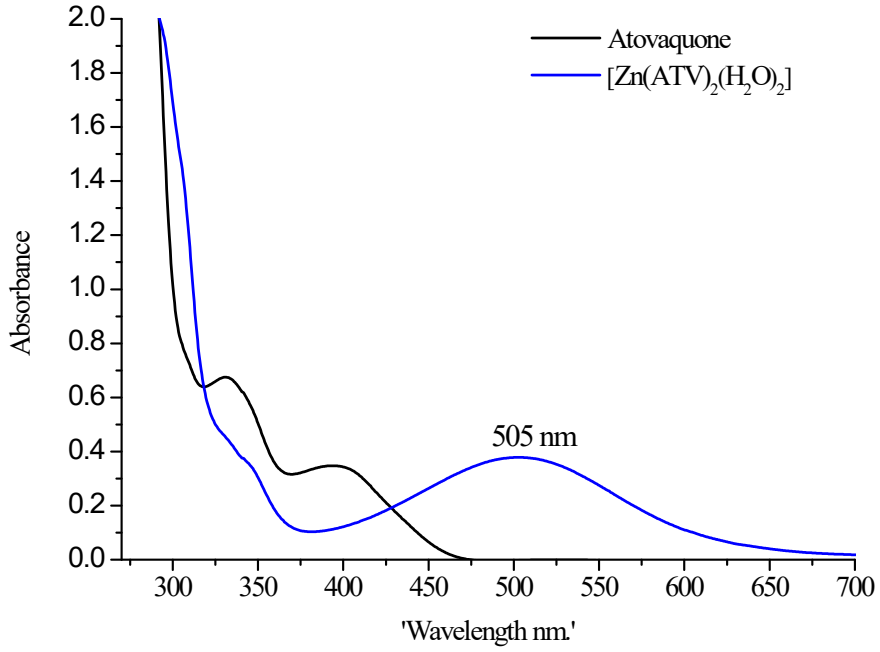

Figure S13: Spectra Uv-Vis of $[Zn(ATV)_2 (H_2O)_2] \cdot 2H_2O$ and ATV in DMSO

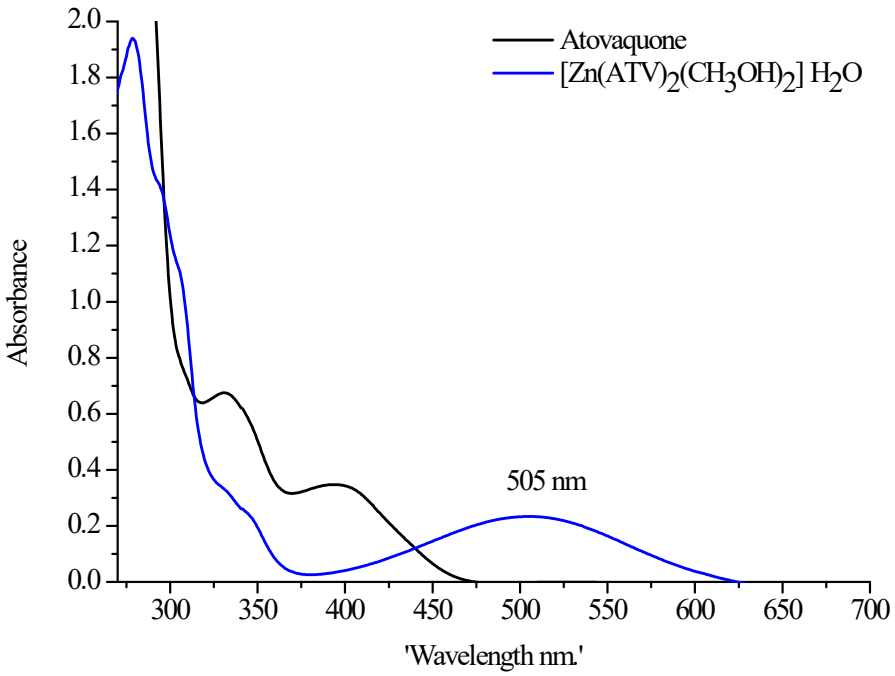

Figure S14: Spectra Uv-Vis of $[Zn(ATV)_2\ (CH_3OH)_2]\ H_2O$ and ATV in DMSO

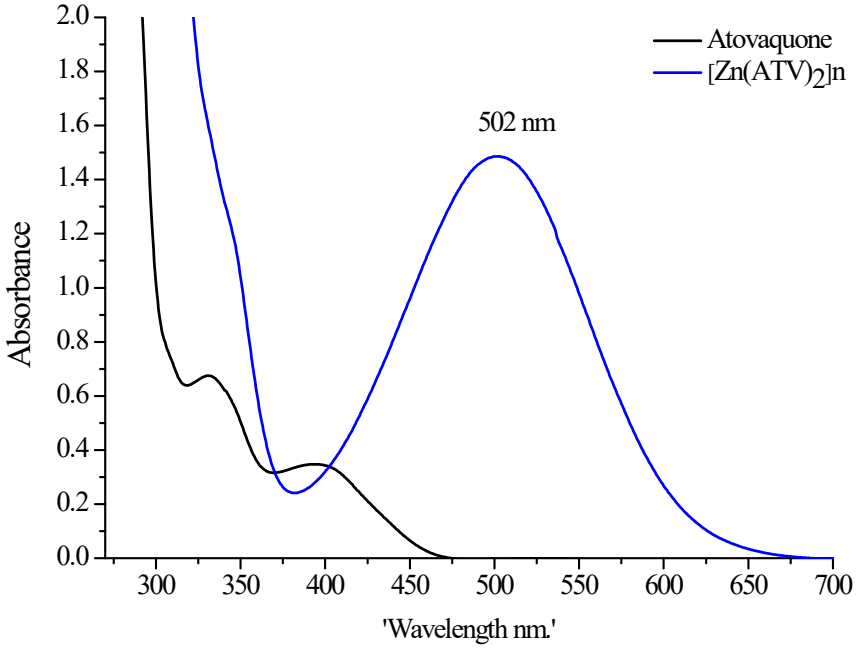

Figure S15: Spectra Uv-Vis of $[Zn(ATV)_2]_n$ and ATV in DMSO

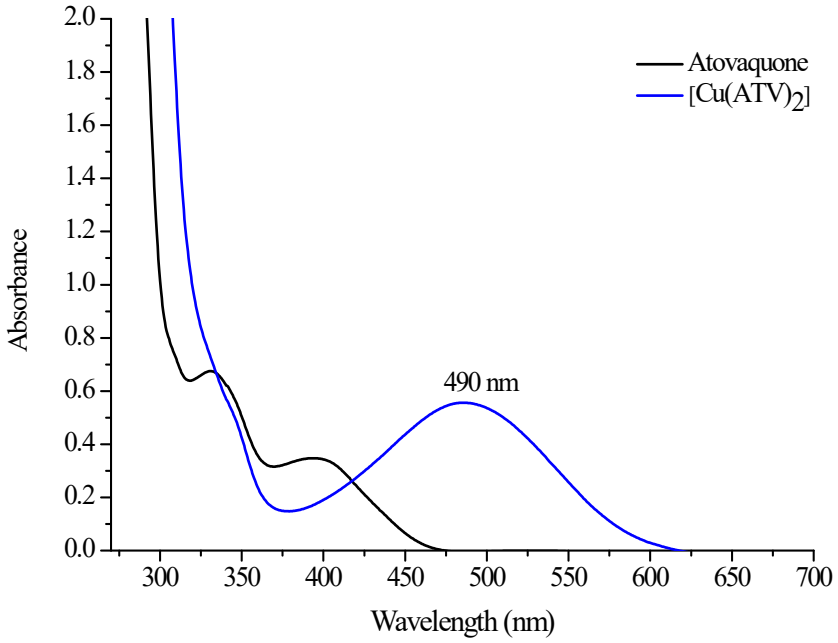

Figure S16: Spectra Uv-Vis of $[Cu(ATV)_2]$ and ATV in DMSO

Characterization by IR spectroscopy

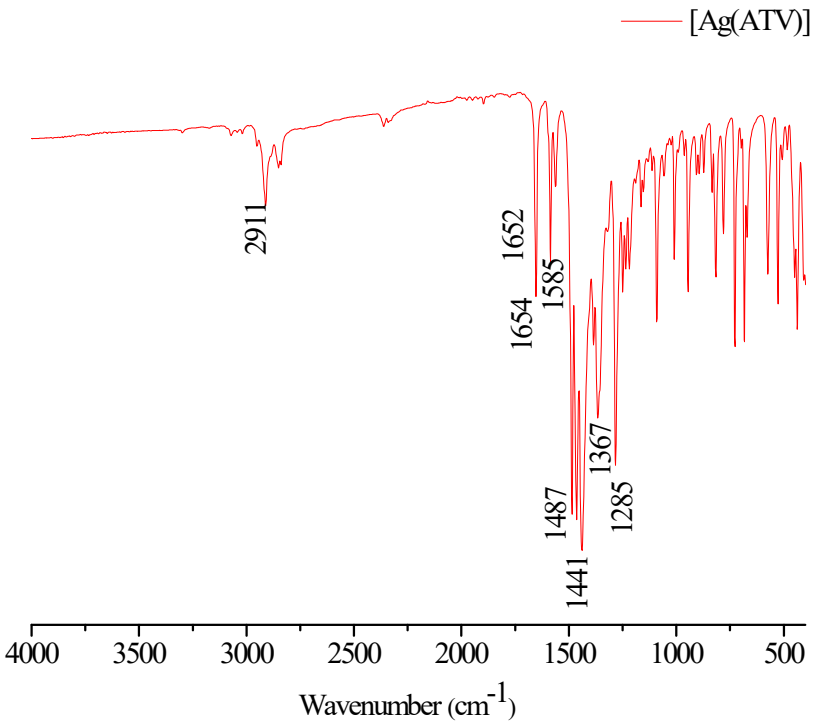

Figure S17: IR Spectrum of [Ag(ATV)]

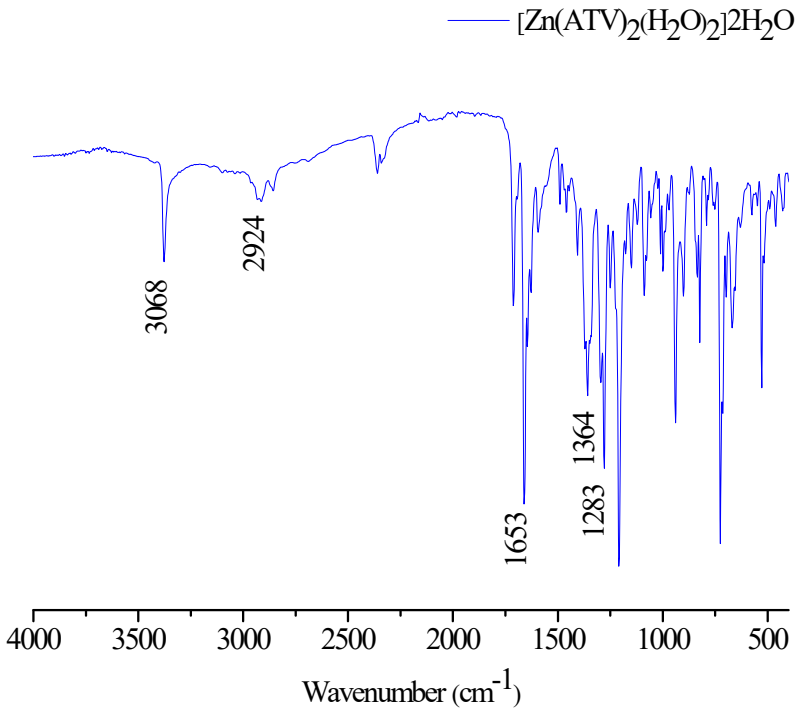

Figure S18: IR spectrum of $[Zn(ATV)_2(H_2O)_2] \cdot 2\ H_2O$

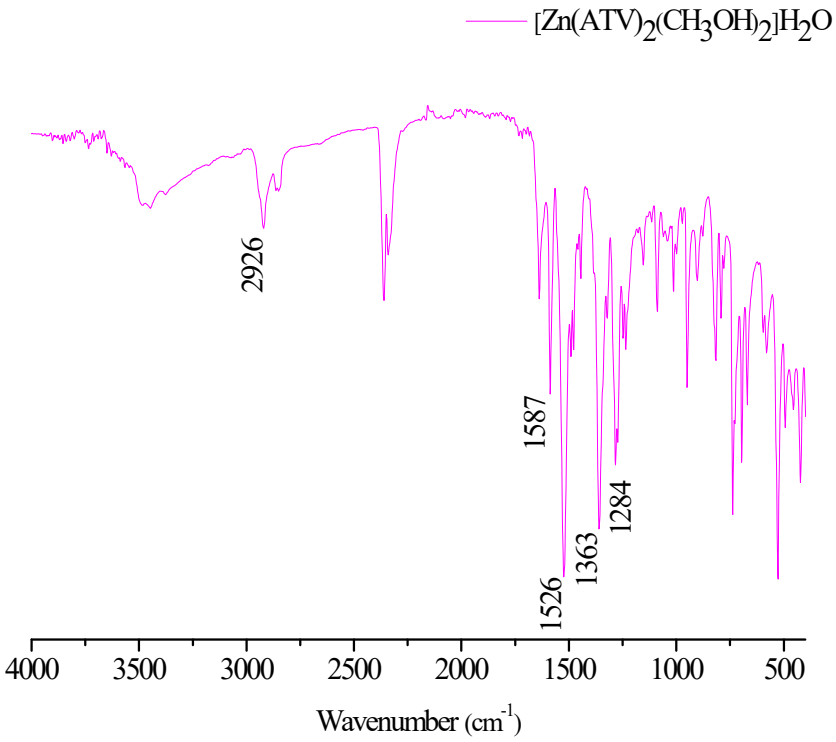

Figure S19: IR spectrum of $[Zn(ATV)_2(CH_3OH)_2] \cdot H_2O$

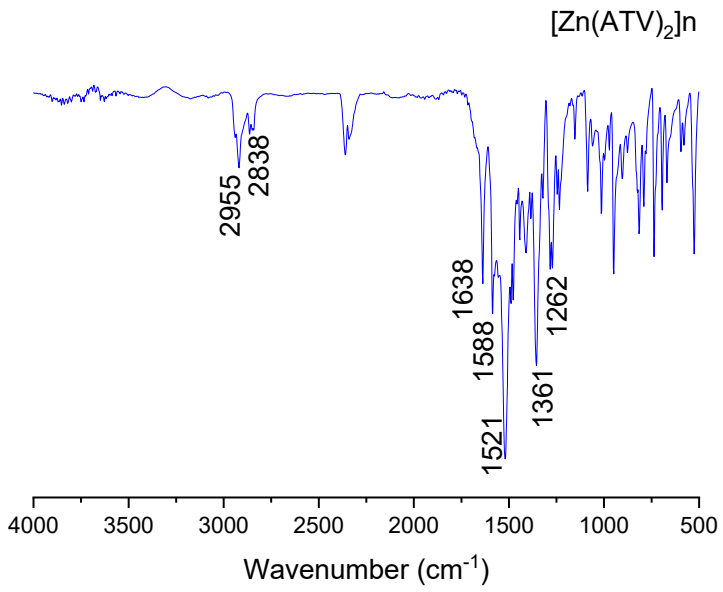

Figure S20: IR spectrum of $[Zn(ATV)_2]n$

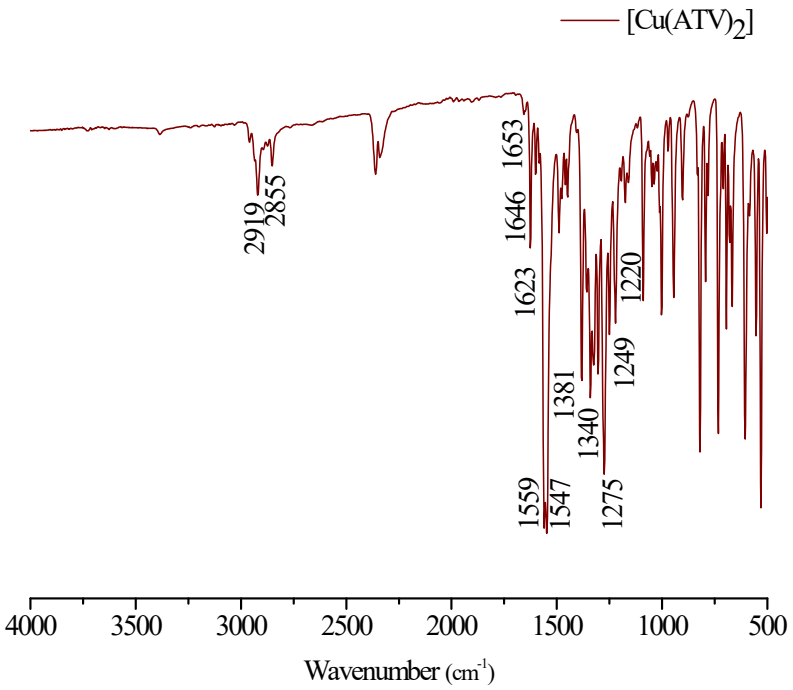

Figure S21: IR Spectrum of $[Cu(ATV)_2]$

Characterization by NRM spectroscopy

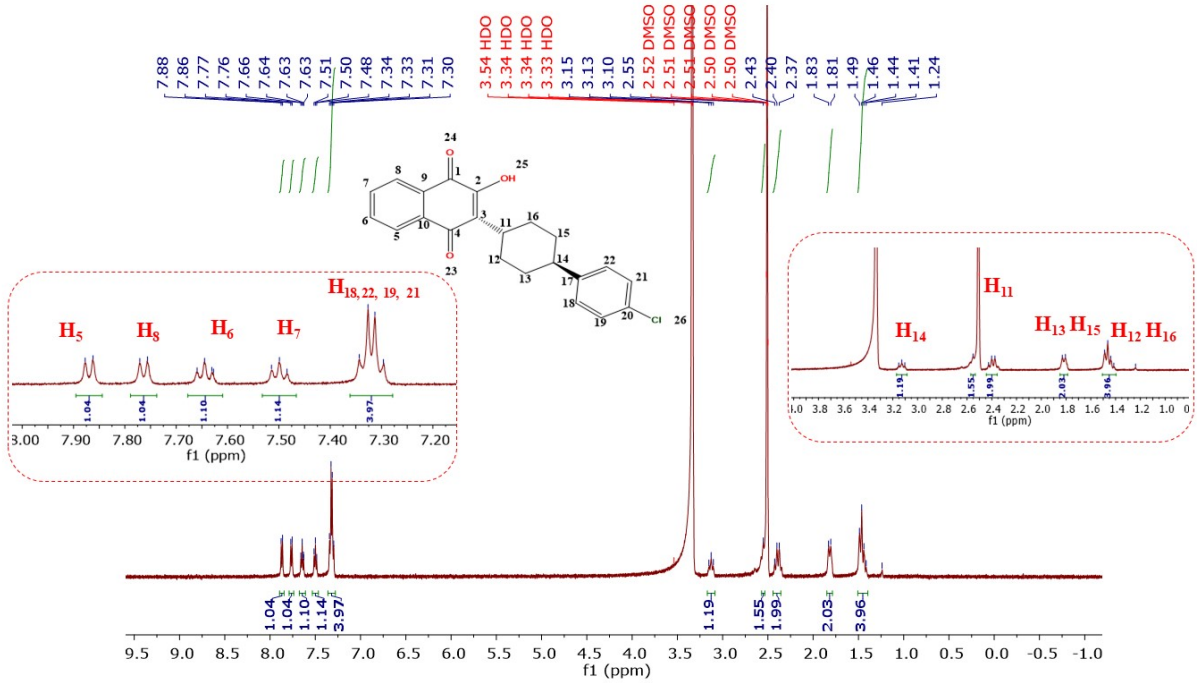

Figure S22: ^{1}H NMR spectrum of the [Ag(ATV)] in DMSO d_6

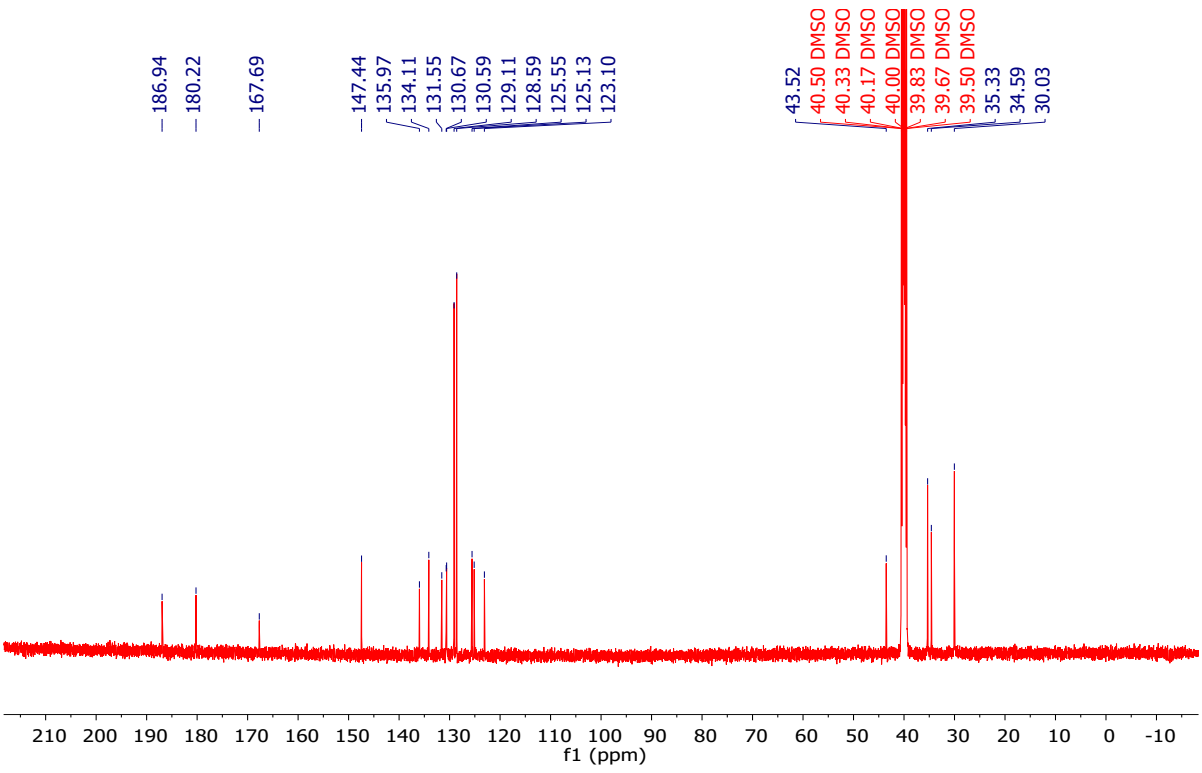

Figure S23: ^{13}C NMR spectrum of the [Ag(ATV)] in DMSO d_6

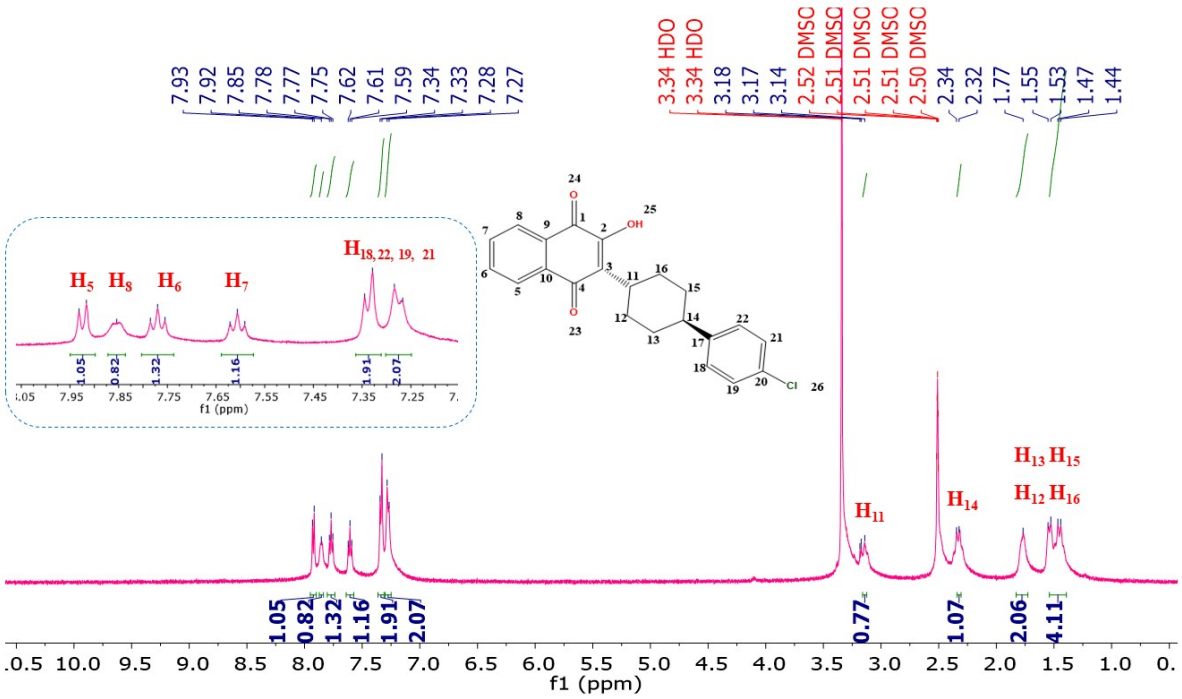

Figure S24: ^{1}H NMR spectrum of the $[Zn(ATV)_2(H_2O)_2]\cdot 2H_2O$ in DMSO-d6

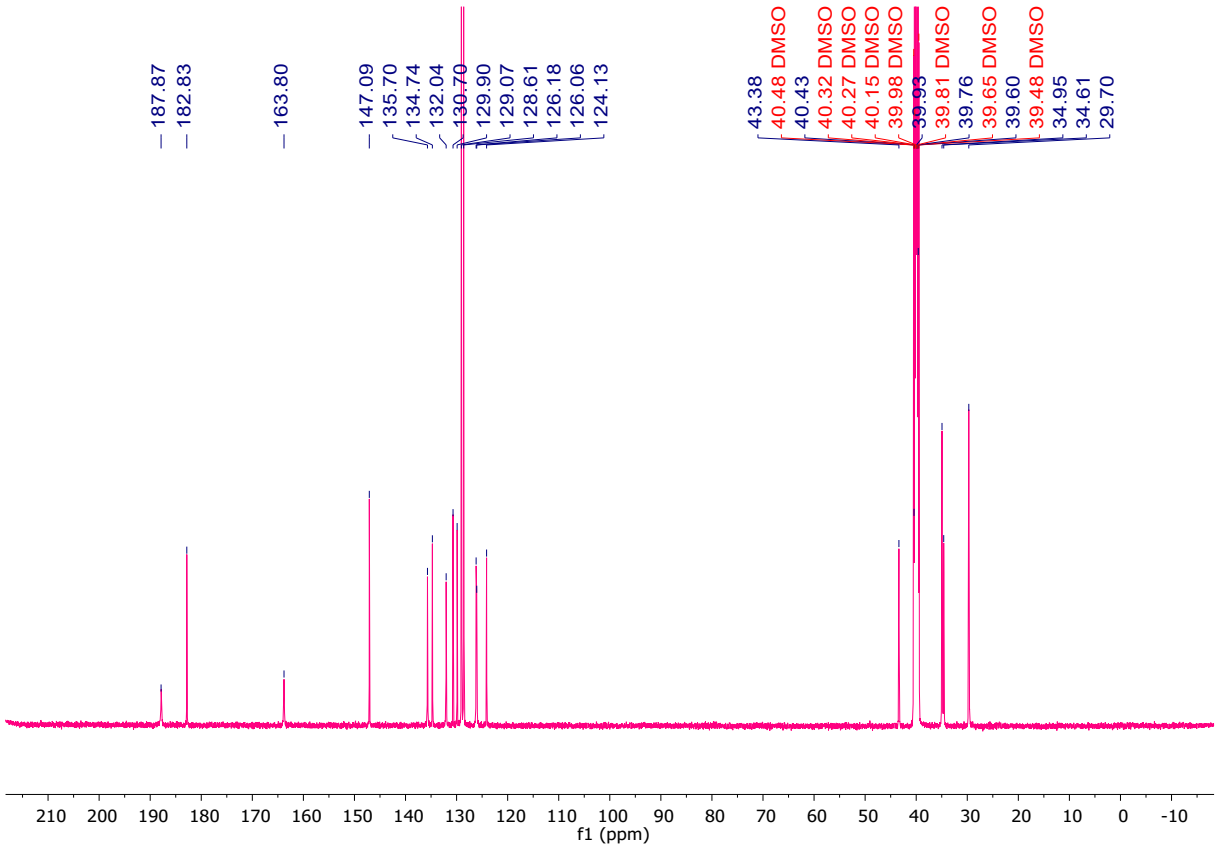

Figure S25: ^{13}C NMR spectrum of the $[Zn(ATV)_2(H_2O)_2]\cdot 2H_2O$ in DMSO-d_6

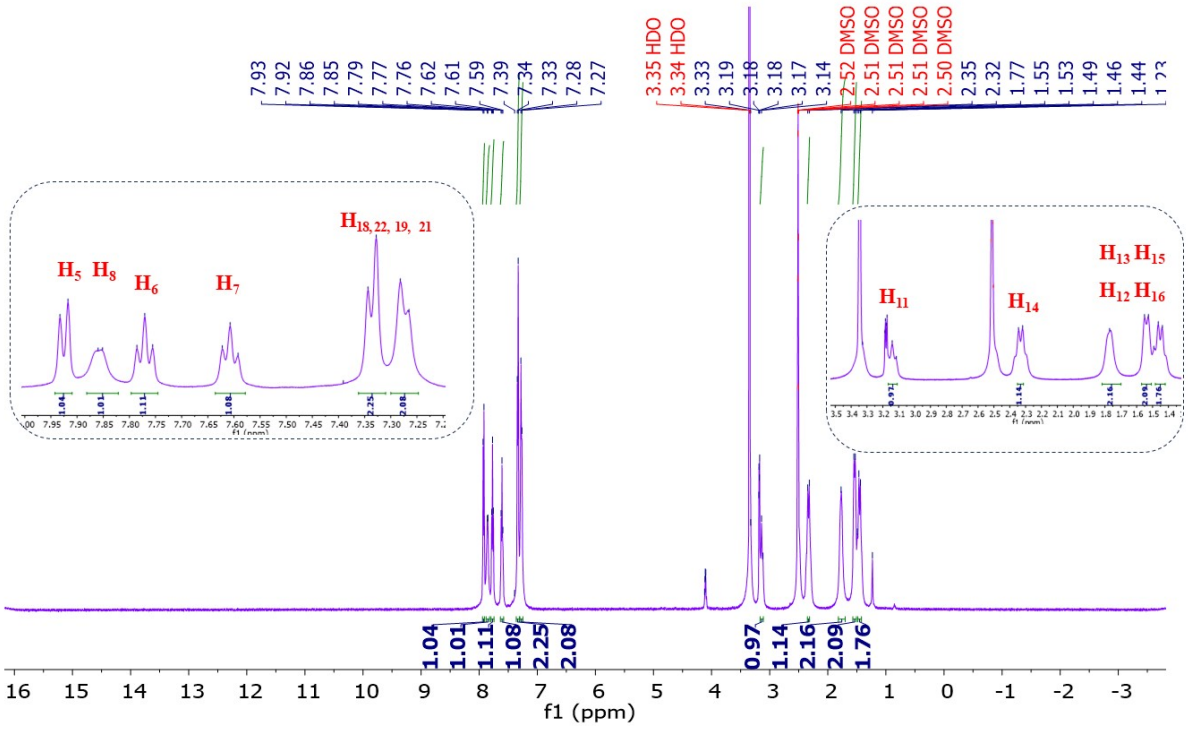

Figure S26: ^{1}H NMR spectrum of the $[Zn(ATV)_2(CH_3OH)_2]\cdot H_2O$ in DMSO-d_6

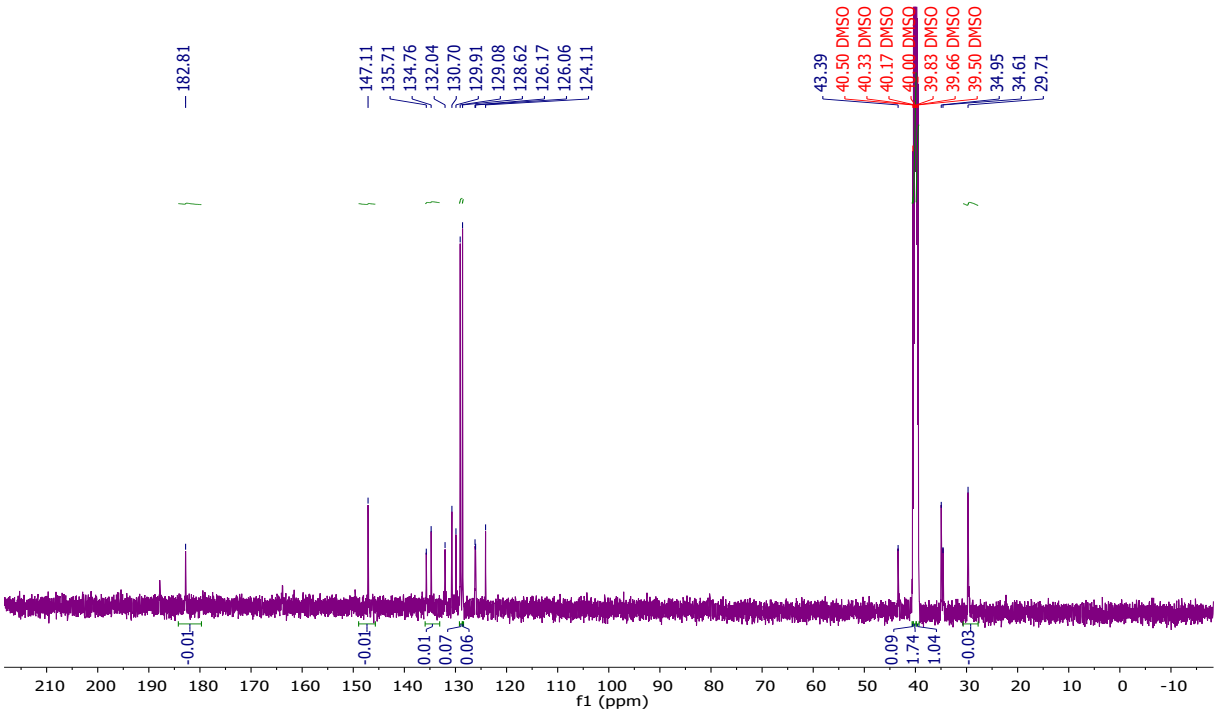

Figure S27: ^{13}C NMR spectrum of the $[Zn(ATV)_2(CH_3OH)_2]\cdot H_2O$ DMSO-d_6

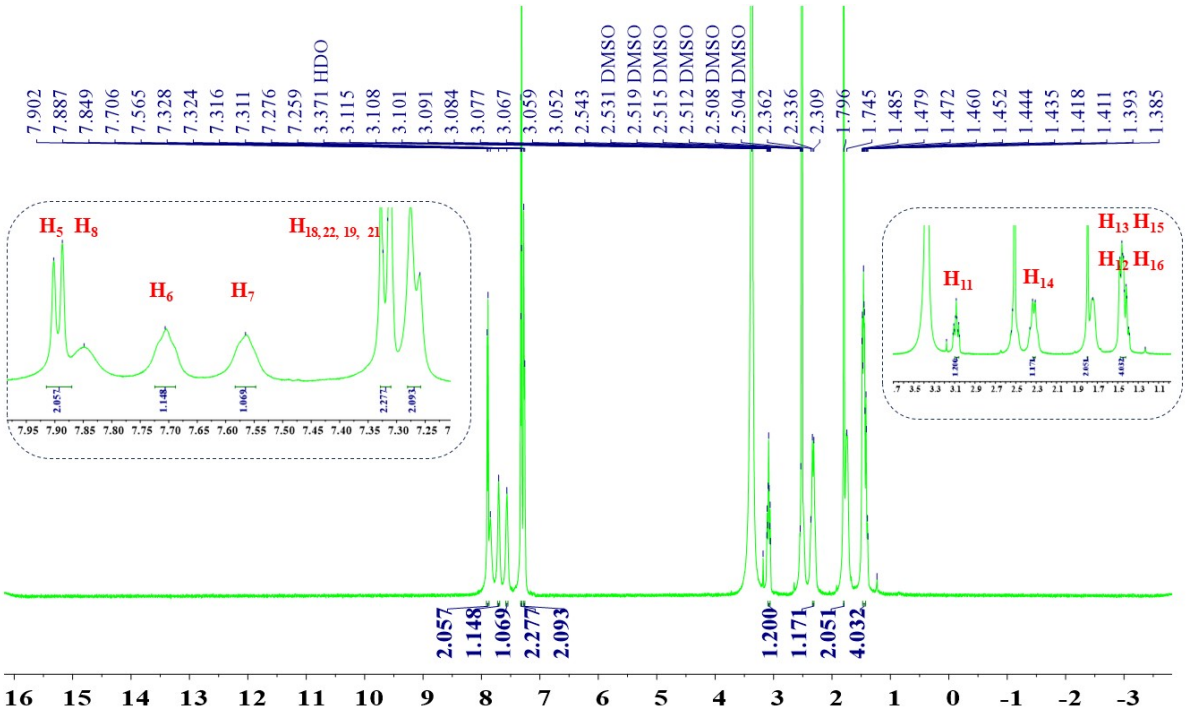

Figure S28: ^{1}H NMR spectrum of the [Zn(ATV)$_2$]n in DMSO-d$_6$

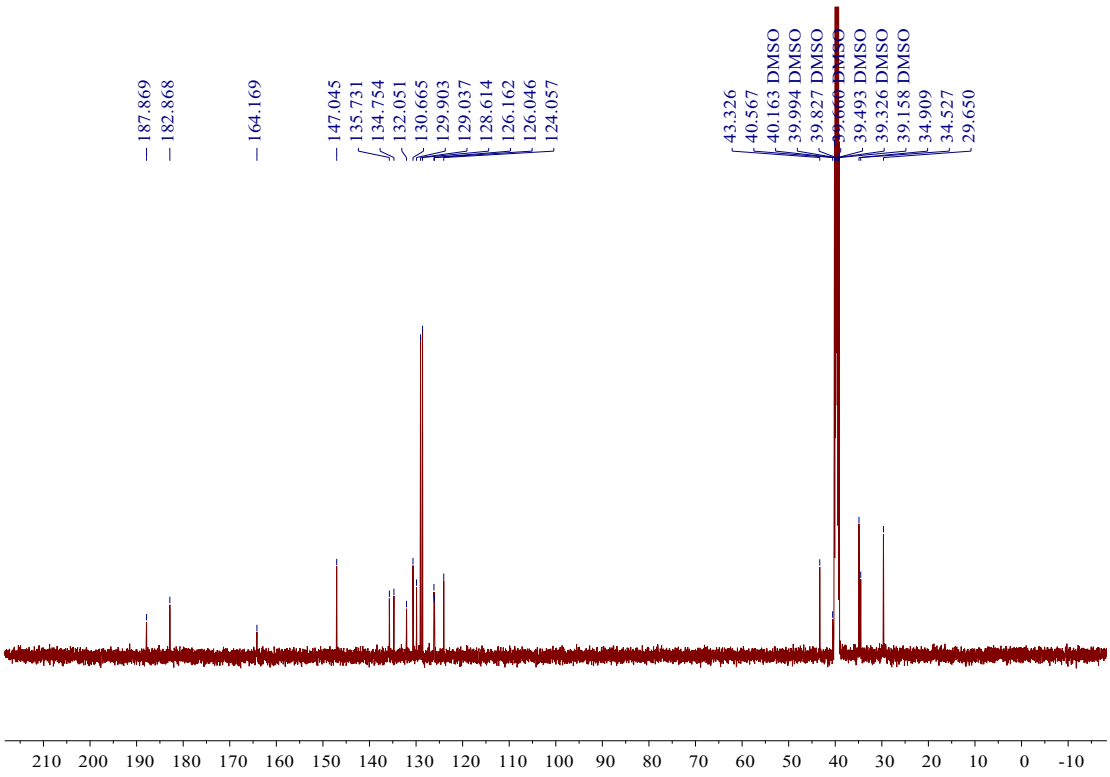

Figure S29: ^{13}C NMR spectrum of the [Zn(ATV)$_2$]n DMSO-d$_6$

Crystallography

X-ray crystallography: Single crystals of {[Zn(ATV)$_2$.(H$_2$O)$_2$]·2H$_2$O} **(2)**, {[Zn(ATV)$_2$.(CH$_3$OH)$_2$]·H$_2$O} **(3)** and {Zn(ATV)$_2$}$_n$ **(4)** were obtained. Suitable crystals were selected and mounted on a Rigaku SuperNova four-circle diffractometer equipped with an AtlasS2 CCD detector at 295 K using Mo-Kα radiation (λ = 0.71073 Å). Multi-scan absorption corrections were applied using the SCALE3 ABSPACK algorithm implemented in CrysAlisPro. The structures were solved using Olex2 software[1], with the SHELXT[2] structure solution program via Intrinsic Phasing, and refined using the SHELXL[2] through Least Squares minimization. C-bound hydrogen atoms were placed in geometrically idealized positions and refined as riding, assuming C—H bond lengths of 0.96 Å for -CH$_2$ and 0.93 Å for aromatic protons, with isotropic displacement parameters Uiso = 1.2Ueq. Water hydrogen atoms were located from difference Fourier maps and refined as rigid units [O—H = 0.85 Å and U_{iso}(H) = 1.5U_{eq}(O)]. For **(2)**, data collection was performed at 291.6(2) K, with 94,901 reflections measured (4.83° ≤ 2Θ ≤ 52.742°), of which 8,600 were unique (Rint = 0.0910, Rsigma = 0.0419). The final refinement converged with R1 = 0.0946 (for I > 2σ(I)) and wR2 = 0.2209 (for all data). For **(3)** was kept at 292.13(16) K during data collection with 78311 reflections measured (4.88° ≤ 2Θ ≤ 52.744°), 8676 unique (R_{int} = 0.0690, R_{sigma} = 0.0354) and final R_1 was 0.0721 (I > 2σ(I)) and wR_2 was 0.1678 (all data). Finally, for **(4)** data collection was performed at 295.26(11) K with 24,563 reflections measured (5.166° ≤ 2Θ ≤ 52.742°), of which 3,719 were unique (Rint = 0.0390, Rsigma = 0.0223) and used in the calculations. The final refinement converged with R1 = 0.0397 (for I > 2σ(I)) and wR2 = 0.1002 (for all data). Crystallographic data for all compounds have been deposited at The Cambridge Crystallographic Data Center (www.ccdc.cam.ac.uk/data_request/cif) and can be obtained free of charge under deposit number: 2495348-2495350.

Table S1. Crystallographic data and refinement parameters for compounds **2-4**.

	2	**3**	**4**
Empirical formula	$C_{44}H_{44}Cl_2O_{10}Zn$	$C_{46}H_{46}Cl_2O_9Zn$	$C_{44}H_{36}Cl_2O_6Zn$
Formula weight	869.06	879.10	797.00
Temperature/K	291.6(2)	292.13(16)	295.26(11)
Crystal system	monoclinic	monoclinic	monoclinic
Space group	$P2_1/n$	$P2_1/n$	$P2_1/c$
a/Å	9.8311(2)	10.1178(3)	14.3365(5)
b/Å	34.9640(9)	33.9796(7)	12.5054(4)
c/Å	12.2263(3)	12.3549(4)	10.2396(3)
α/°	90	90	90
β/°	91.199(2)	90.635(3)	97.263(3)
γ/°	90	90	90
Volume/Å^3	4201.68(17)	4247.3(2)	1821.06(10)
Z	4	4	2
ρ_{calc}g/cm^3	1.374	1.375	1.453
μ/mm^{-1}	0.769	0.760	0.872
F(000)	1808.0	1832.0	824.0
Crystal size/mm^3	0.35 × 0.277 × 0.07	0.96 × 0.56 × 0.35	0.56 × 0.45 × 0.14
2Θ range for data collection/°	4.83 to 52.742	4.88 to 52.744	5.166 to 52.742
Reflections collected	94901	78311	24563
Independent reflections	8600	8676	3719
Data/restraints/parameters	8600/0/522	8676/0/528	3719/0/241
Goodness-of-fit on F^2	1.131	1.096	1.049
Final R indexes [I>=2σ (I)]	R_1 = 0.0946, wR_2 = 0.2060	R_1 = 0.0721, wR_2 = 0.1565	R_1 = 0.0397, wR_2 = 0.0956
Largest diff. peak/hole / e Å^{-3}	1.33/-0.43	0.57/-0.44	0.44/-0.35

Table S2: Bond parameters for compound **2**.

Atom	***Atom***	***Atom***	***Length (Å)***	***SA (%)***	***S (Å^2)***
Zn	O2		2.1651(15)	15.76	4.36
Zn	O2^{i}		2.1650(15)		
Zn	O1^{i}		1.9492(14)	18.88	4.91
Zn	O1		1.9492(14)		
Zn	O3^{ii}		2.2345(15)	15.09	4.22
Zn	O3^{iii}		2.2345(15)		
			Angle (°)		
O2^{i}	Zn	O2	180		
O2	Zn	O3^{ii}	94.70(6)		
O2	Zn	O3^{iii}	85.30(6)		
O2^{i}	Zn	O3^{ii}	85.30(6)		
O2^{i}	Zn	O3^{iii}	94.70(6)		
O1^{i}	Zn	O2^{i}	79.55(6)		
O1	Zn	O2^{i}	100.45(6)		
O1	Zn	O2	79.55(6)		
O1^{i}	Zn	O2	100.45(6)		
O1^{i}	Zn	O1	180		
O1^{i}	Zn	O3^{iii}	89.07(6)		
O1^{i}	Zn	O3^{ii}	90.93(6)		
O1	Zn	O3^{iii}	90.93(6)		
O1	Zn	O3^{ii}	89.07(6)		
O3^{ii}	Zn	O3^{ii}	180.00(4)		

Symmetry operations: (i) 1-X,-Y,1-Z; ***(ii)*** +X,1/2-Y,1/2+Z; ***(iii)*** 1-X,-1/2+Y,1/2-Z

Table S3: Bond parameters for compound **3**.

Atom	***Atom***	***Atom***	***Length (Å)***
Zn	O3		2.006(4)
Zn	O1		1.974(4)
Zn	O2		2.275(4)
Zn	O4		2.199(4)
Zn	O6		2.129(5)
Zn	O5		2.078(5)
			Angle (º)
O3	Zn	O2	87.46(15)
O3	Zn	O4	77.26(15)
O3	Zn	O6	101.43(18)
O3	Zn	O5	97.4(2)
O1	Zn	O3	154.34(17)
O1	Zn	O2	76.21(15)
O1	Zn	O4	86.45(16)
O1	Zn	O6	96.30(19)
O1	Zn	O5	101.5(2)
O4	Zn	O2	100.98(17)
O6	Zn	O2	83.49(18)
O6	Zn	O4	175.23(19)
O5	Zn	O2	171.3(2)
O5	Zn	O4	87.2(2)
O5	Zn	O6	88.5(2)
C23	O3	Zn	118.2(3)
C1	O1	Zn	120.0(3)
C2	O2	Zn	110.1(3)
C24	O4	Zn	111.9(4)

Table S4: Bond parameters for compound **4**.

Atom	*Atom*	*Atom*	*Length (Å)*
Zn	O2		1.965(2)
Zn	O4		1.945(3)
Zn	O3		2.297(3)
Zn	O1		2.280(3)
Zn	O5		2.084(3)
Zn	O6		2.073(3)
			Angle (º)
O2	Zn	O3	88.77(10)
O2	Zn	O1	76.00(11)
O2	Zn	O5	98.20(12)
O2	Zn	O6	99.07(14)
O4	Zn	O2	153.11(12)
O4	Zn	O3	76.32(10)
O4	Zn	O1	86.74(12)
O4	Zn	O5	102.50(13)
O4	Zn	O6	99.11(14)
O1	Zn	O3	106.34(11)
O5	Zn	O3	84.79(13)
O5	Zn	O1	167.11(13)
O6	Zn	O3	169.11(14)
O6	Zn	O1	83.02(16)
O6	Zn	O5	86.61(18)
C6	O2	Zn	120.7(2)
C28	O4	Zn	120.9(2)
C23	O3	Zn	109.4(2)
C1	O1	Zn	110.5(3)

Table S5: Hydrogen Bonds for compounds **2** and **3**.

D	**H**	**A**	**d(D-H) (Å)**	**d(H-A) (Å)**	**d(D-A) (Å)**	**D-H-A (°)**
Compound 02						
O6	H6A	O8[1]	0.85	2.01	2.854(6)	170.6
O5	H5A	O10	0.85	1.91	2.749(9)	167.9
O5	H5B	O9	0.85	2.00	2.818(13)	159.9
O10	H10A	O7[2]	0.85	1.94	2.768(7)	165.0
O9	H9B	O8[1]	0.85	1.87	2.703(10)	166.9
Compound 03						
O5	H5	O8[i]	0.82	1.97	2.767(4)	165.1
O6	H6	O7	0.82	1.85	2.664(6)	170.5
O7	H7A	O9[iii]	0.85	1.89	2.718(5)	165.9

[i] 1-X,1-Y,1-Z; [ii] 1/2+X,1/2-Y,-1/2+Z; [iii] -1/2+X,1/2-Y,-1/2+Z

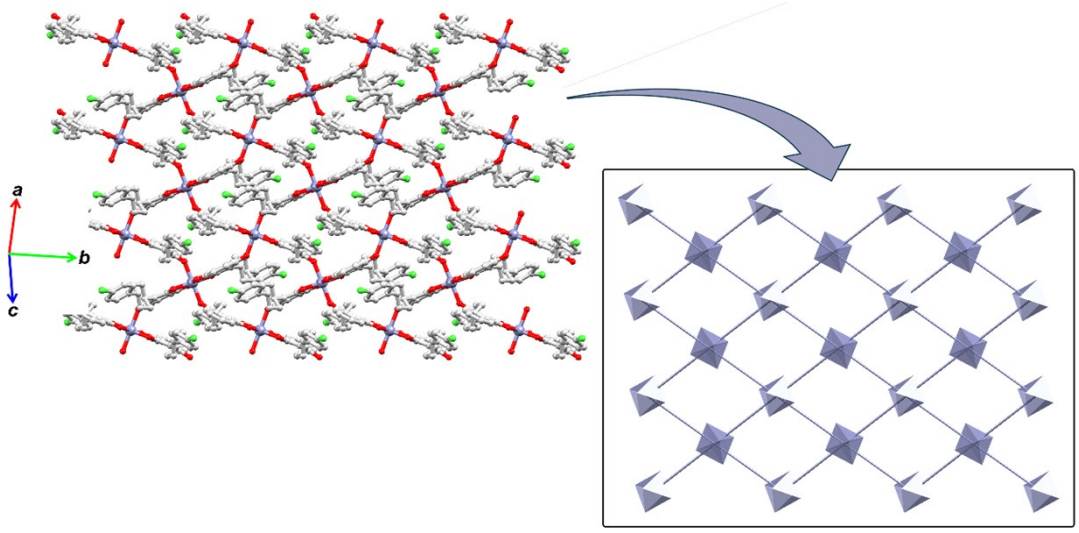

Figure S30: 2D framework representation for compound **4**. In **(a)** 2D coordination polymer representation and **(b)** topological simplification with polyhedral representation of metal centers.

Computational methods and results

Computational methods and results: A preliminary computational study was conducted to optimize the crystal structure of compound **1** using the B3LYP functional with the 6-31G(d,p) basis set. The calculations, performed with the Gaussian09 suite[3], were based on similar metal-based compounds[4,5]. The structural parameters, including bond lengths and angles, were determined from the optimized geometries and compared with experimental values obtained from X-ray crystallography data. The average Zn–O bond length calculated was 1.9647 Å. Quantum chemical descriptors for compound **1** show the stability, suggesting that it does not undergo decomposition and favoring tetrahedral geometry.

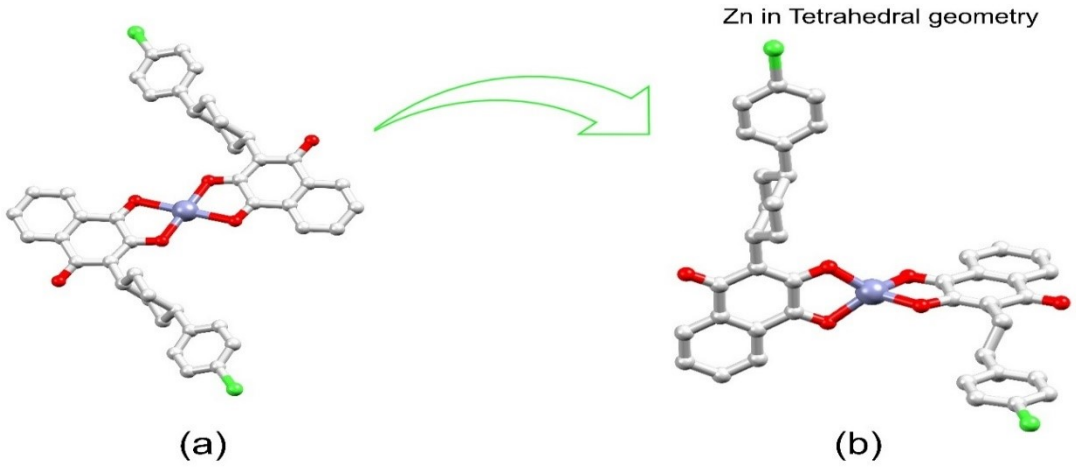

Figure S31: (a) Crystal structure of compound **4** without axial bonds before geometric optimization (input). (b) B3LYP/6-31G(d,p)-optimized geometry of compound **4.**

Table S6: Quantum chemical descriptors for compound **4** in vacuum.

1	
E_{HOMO} (eV)	−4.970
E_{LUMO} (eV)	−2.803
ΔE_{gap}(eV)	2.167
μ (eV)	−3.886
η (eV)	1.083
S (eV)	0.461
X (eV)	3.886
ω (eV)	6.971

Symbols: μ: chemical potential, η: hardness value, S: softness, χ: electronegativity, ω: electrophilicity index. All parameters are expressed by the equations [6].

Experimental studies on the stability of metal complexes in solution

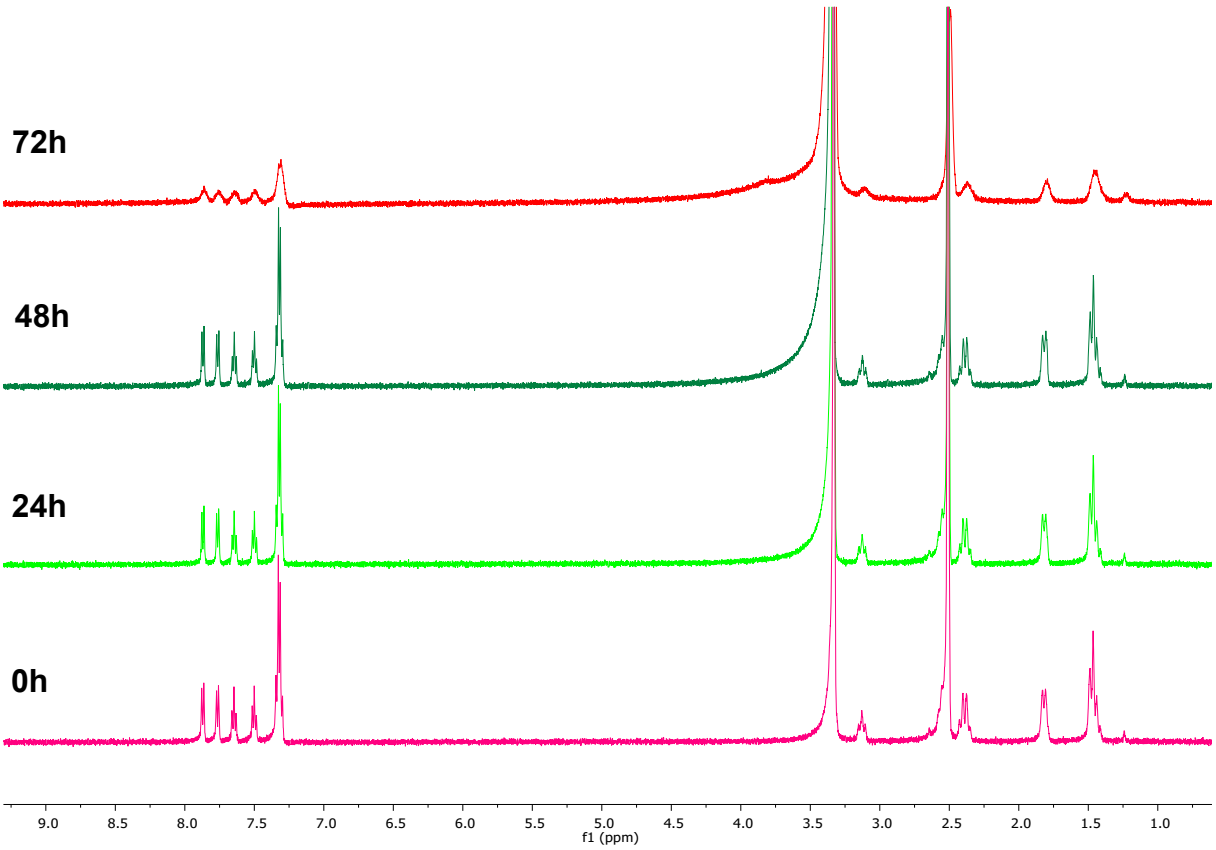

Figure S32: Stability study by ^{1}H NMR of [Ag(ATV)] in DMSO-d_6 (72h)

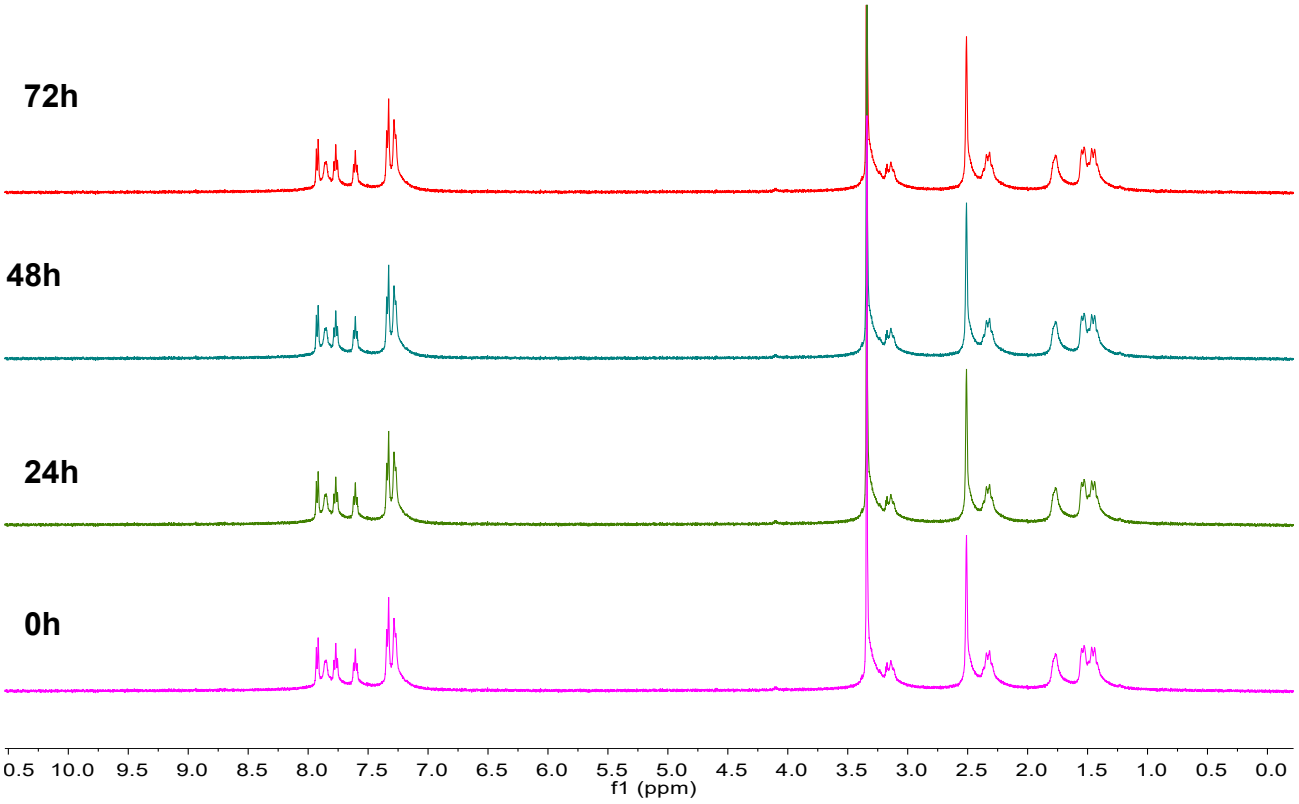

Figure S33: Stability study by ^{1}H NMR of $[Zn(ATV)_2(H_2O)_2]\cdot 2H_2O$ in DMSO-d_6 (72h)

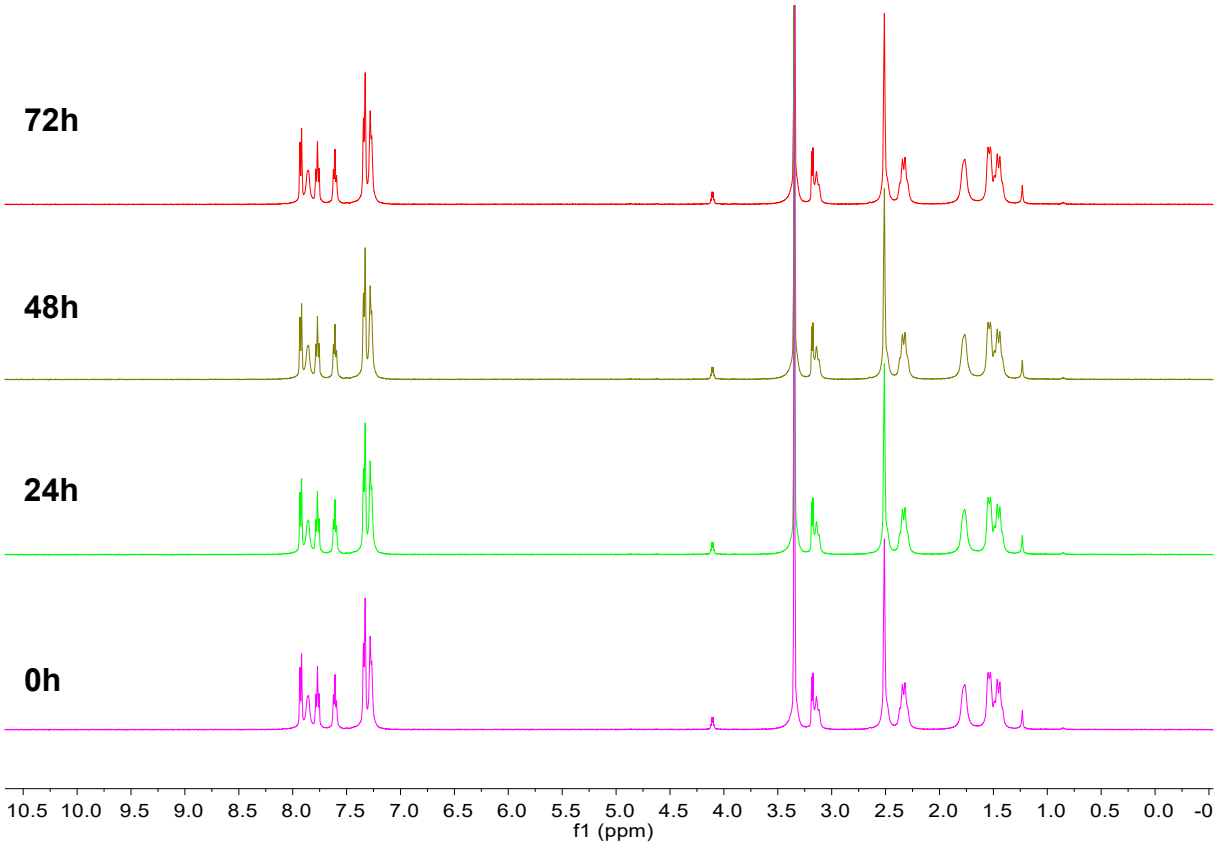

Figure S34: Stability study by ^{1}H NMR $[Zn(ATV)_2(CH_3OH)_2]\cdot H_2O$ in DMSO-d_6 (72h)

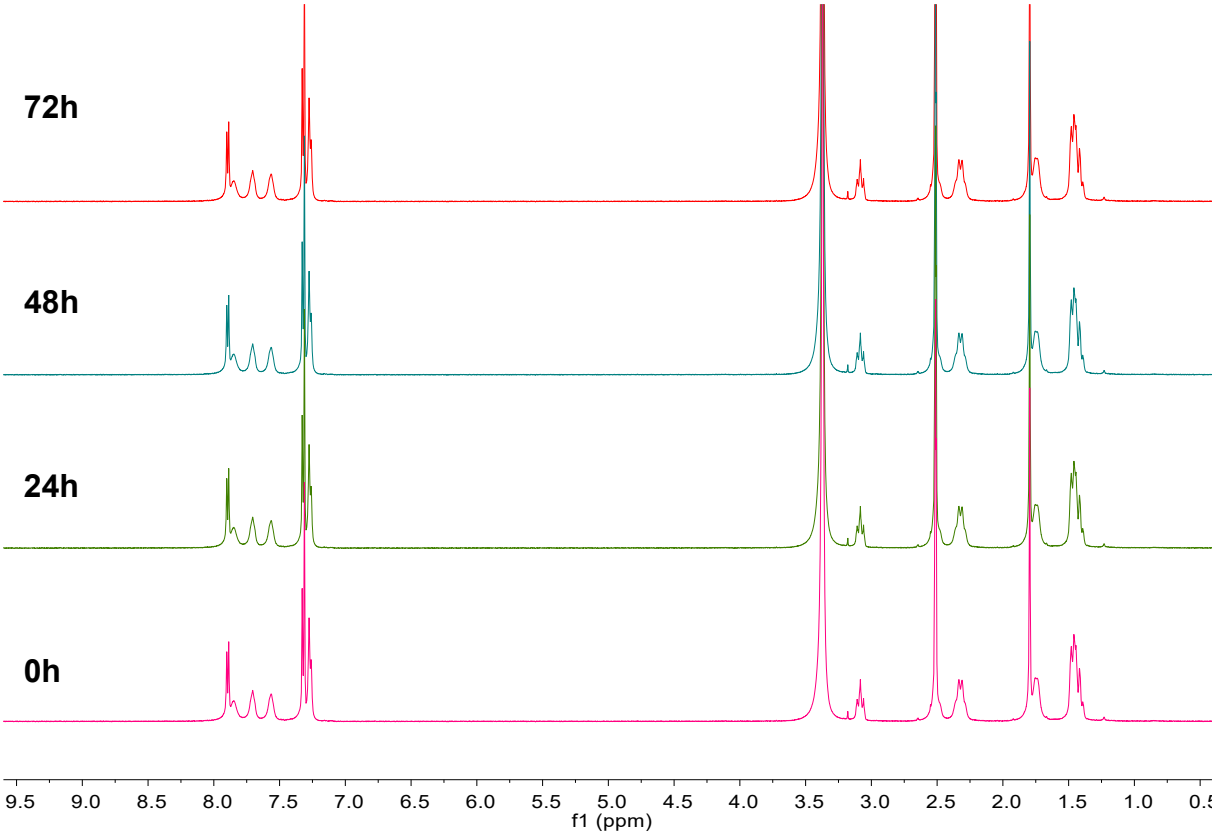

Figure S35: Stability study by ^{1}H NMR of $[Zn(ATV)_2]$ in DMSO-d_6 (72h)

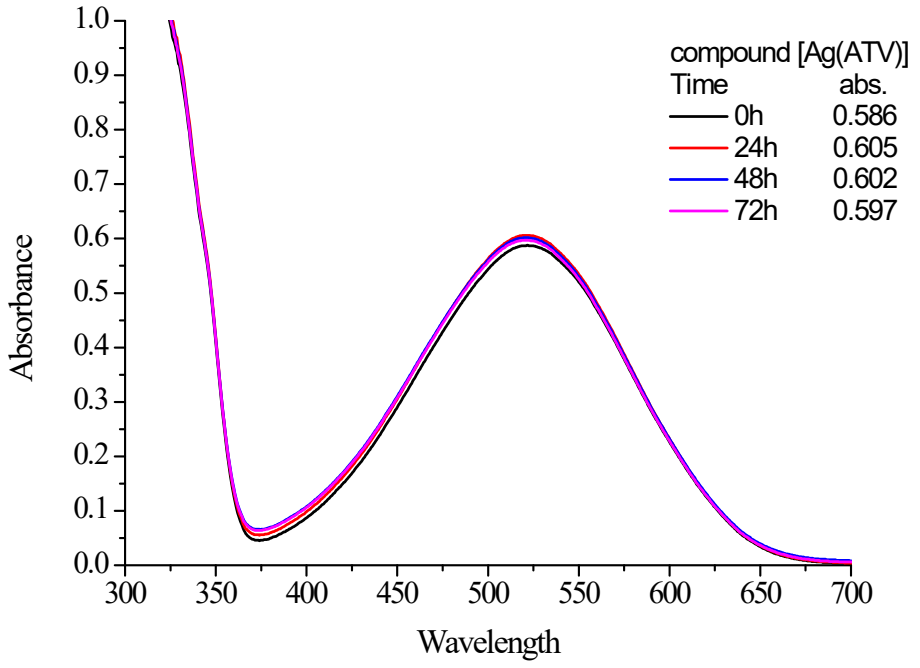

Figure S36: Stability study by Uv-Vis of [Ag(ATV), compound **1** in DMSO (72h)

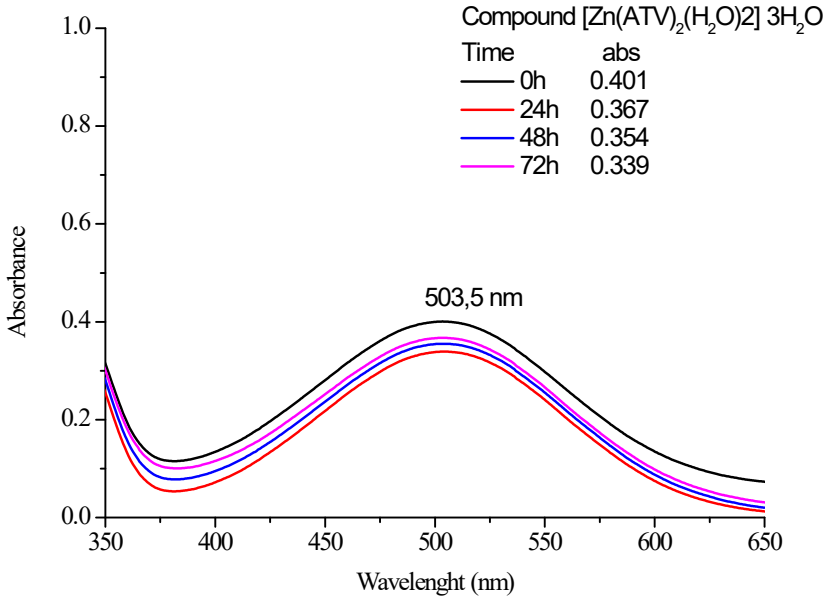

Figure S37: Stability study by Uv-Vis of $[Zn(ATV)_2 (H_2O)_2]\cdot 2\ H_2O$, compound **2** in DMSO (72h)

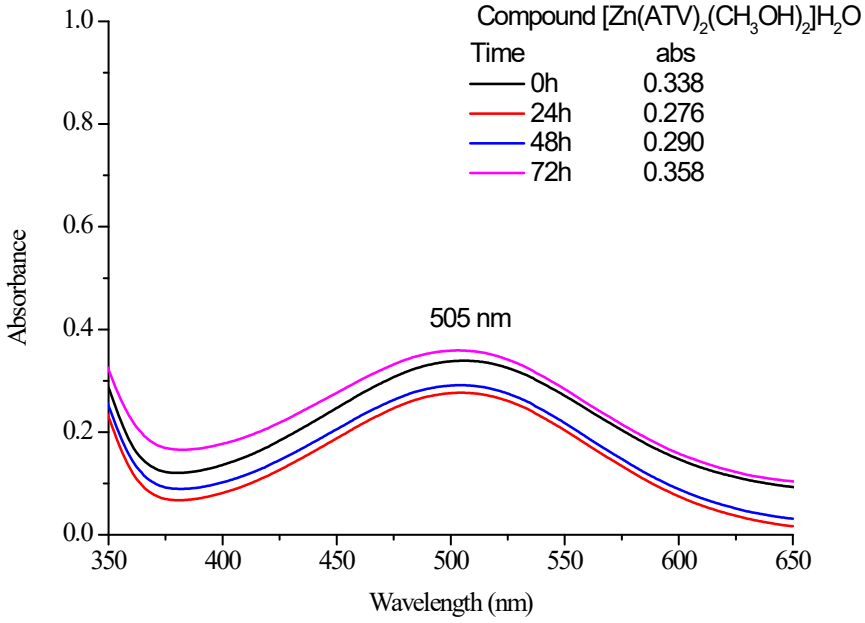

Figure S38: Stability study by Uv-Vis of $[Zn(ATV)_2(CH_3OH)_2]\cdot H_2O$, compound 3 in DMSO (72h)

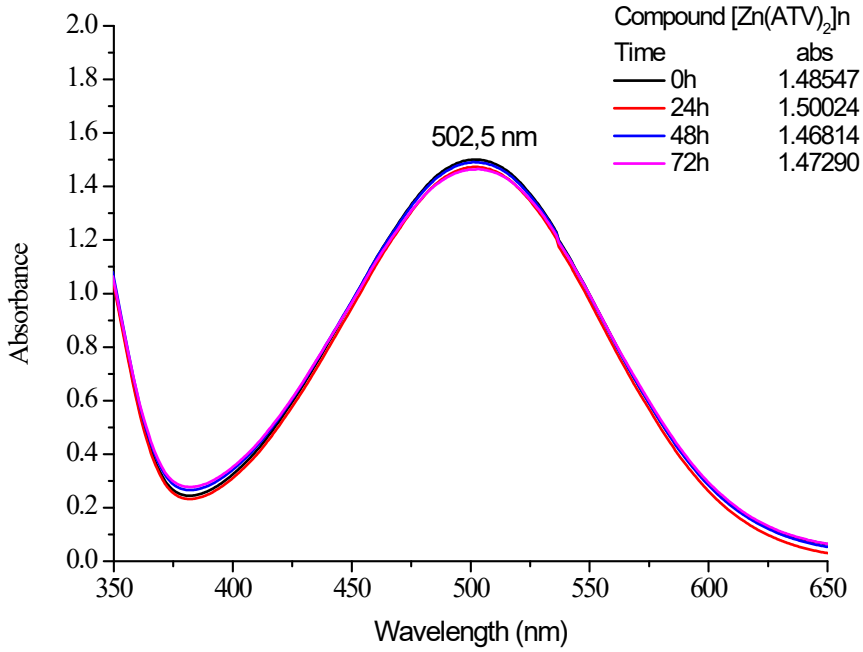

Figure S39: Stability study by Uv-Vis of $\{Zn(ATV)_2\}_n$, compound 4 in DMSO (72h)

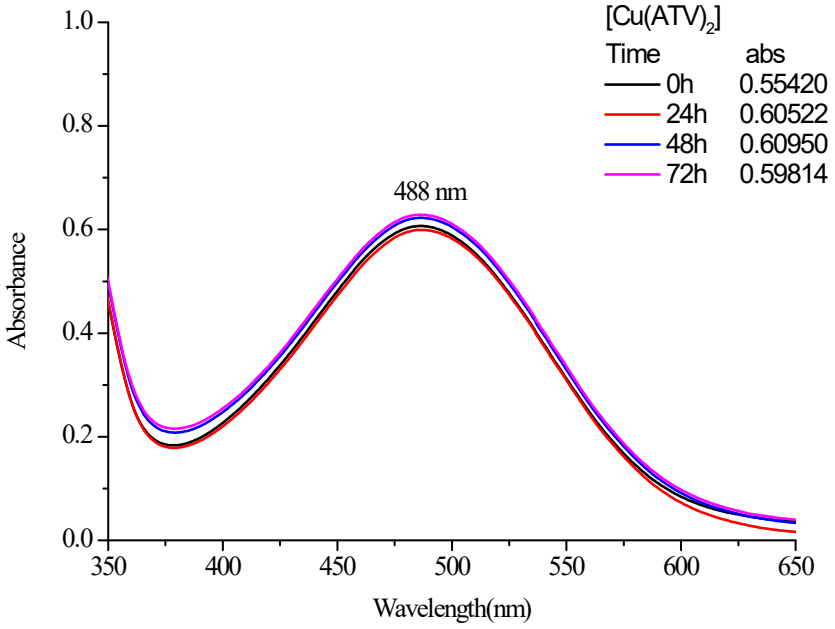

Figure S40: Stability study by Uv-Vis of [Cu(ATV)$_2$], compound **5** in DMSO (72h)

Interaction studies with ferriprotoporphyrin IX

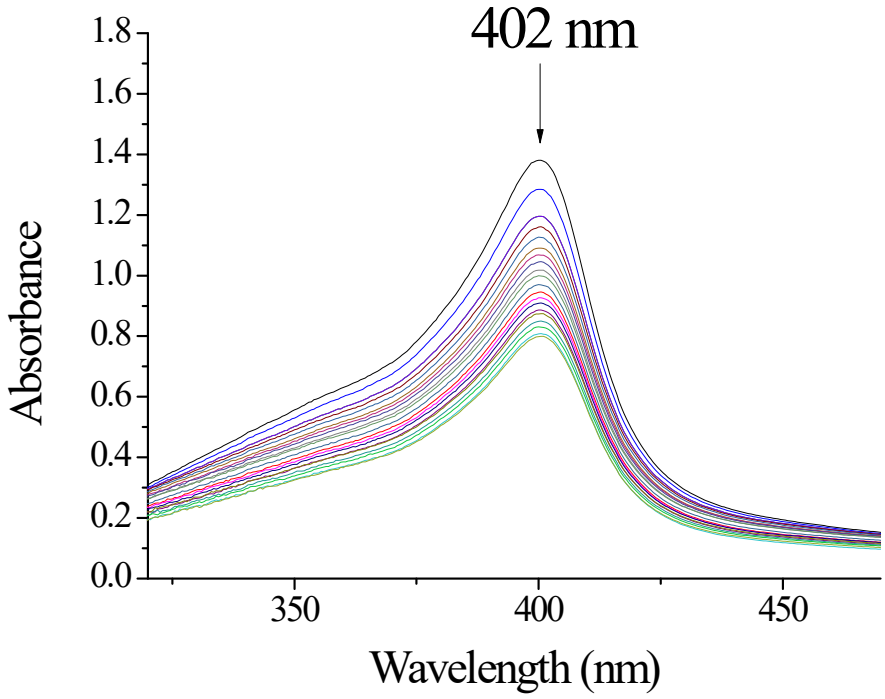

Figure S41: Interaction of [Ag(ATV)] compound **1** with ferriprotoporphyrin

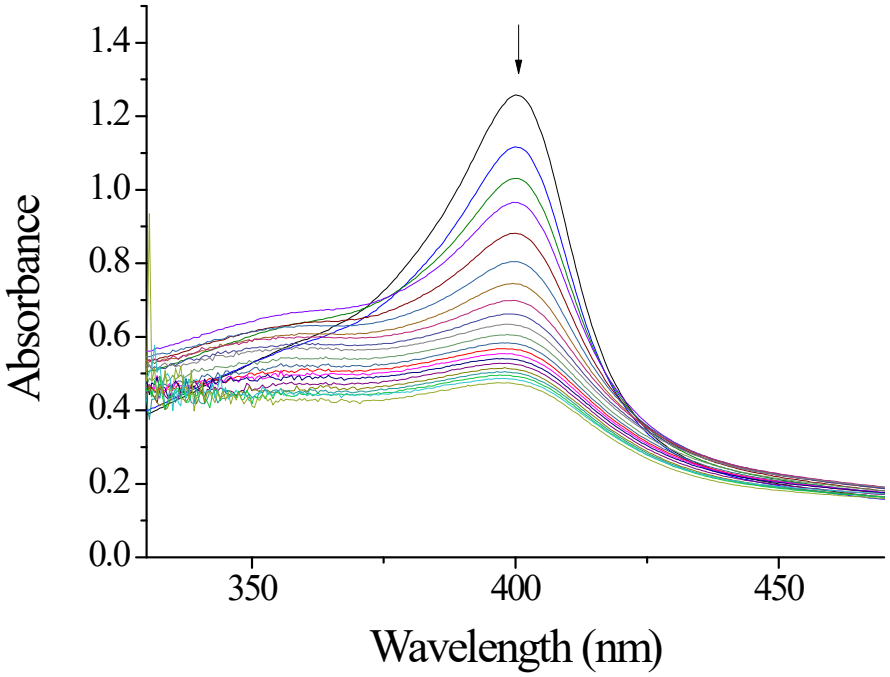

Figure S42: Interaction of $[Zn(ATV)_2(H_2O)_2]\cdot 2H_2O$ compound **2** with ferriprotoporphyrin

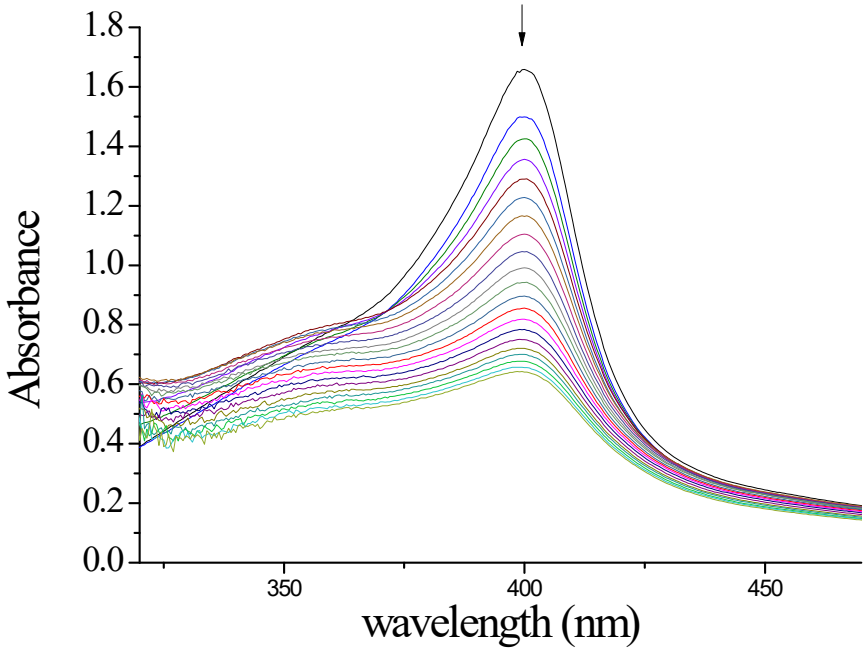

Figure S43: Interaction of $[Zn(ATV)_2(CH_3OH)_2]\cdot H_2O$ compound **3** with ferriprotoporphyrin

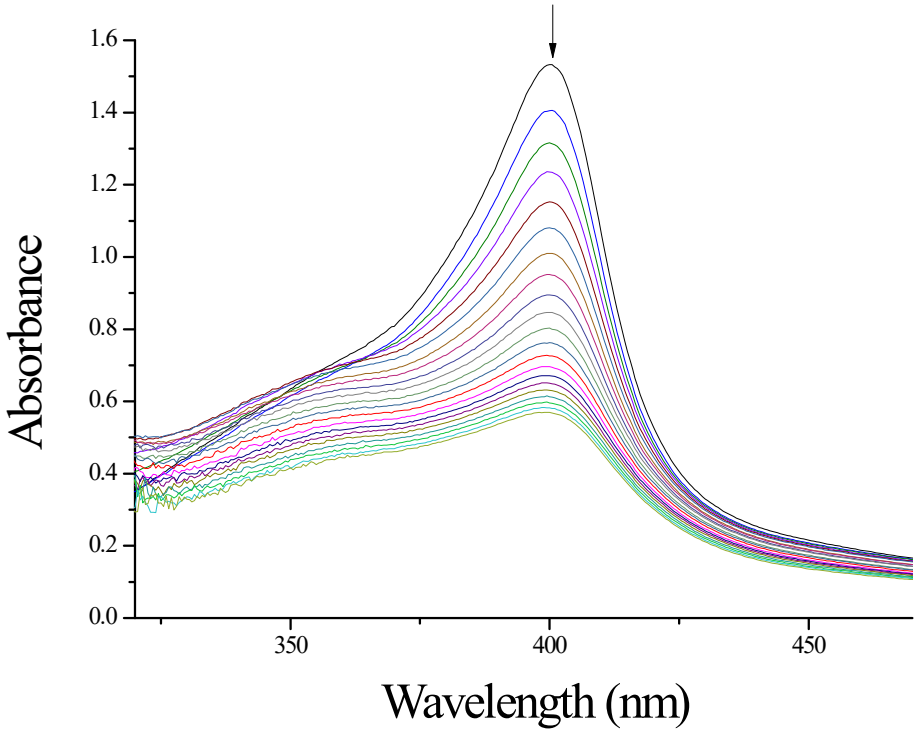

Figure S44: Interaction of $[[Zn(ATV)_2]_n$ compound **4** with ferriprotoporphyrin

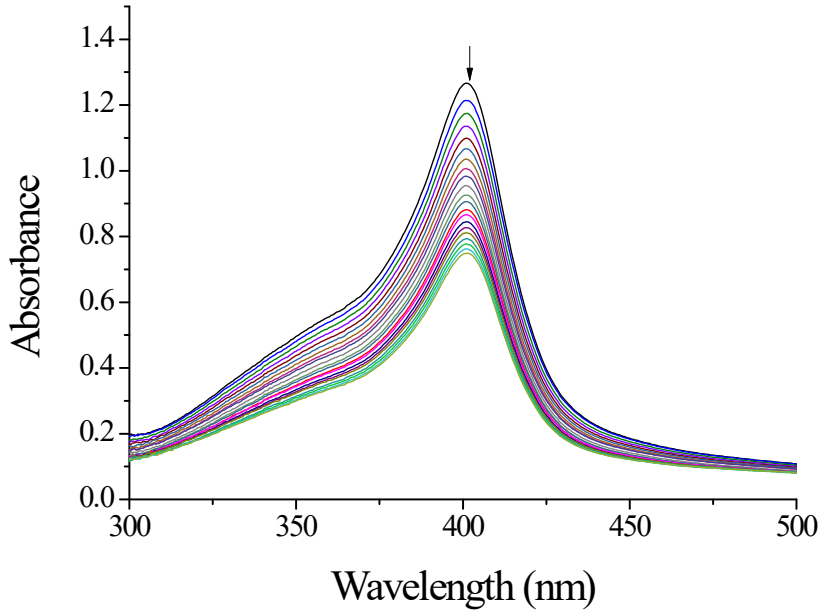

Figure S45: Interaction of [Cu(ATV)$_2$] compound **5** with ferriprotoporphyrin

Studies on the inhibition of β-hematin formation

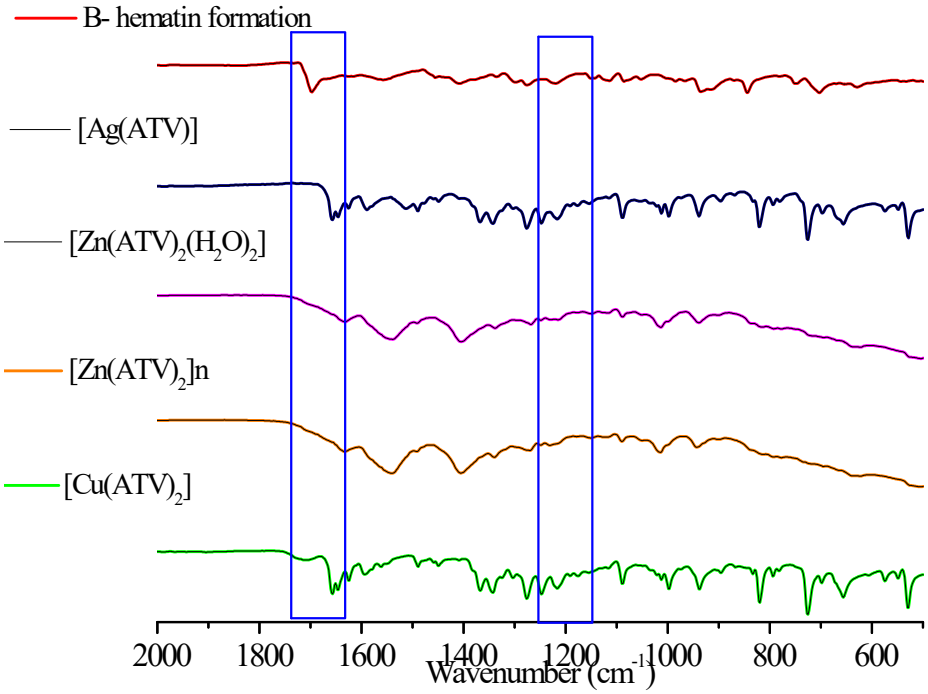

Figure S46: Spectra ß-hematin formation and inhibition of β-hematin formation to metal complexes

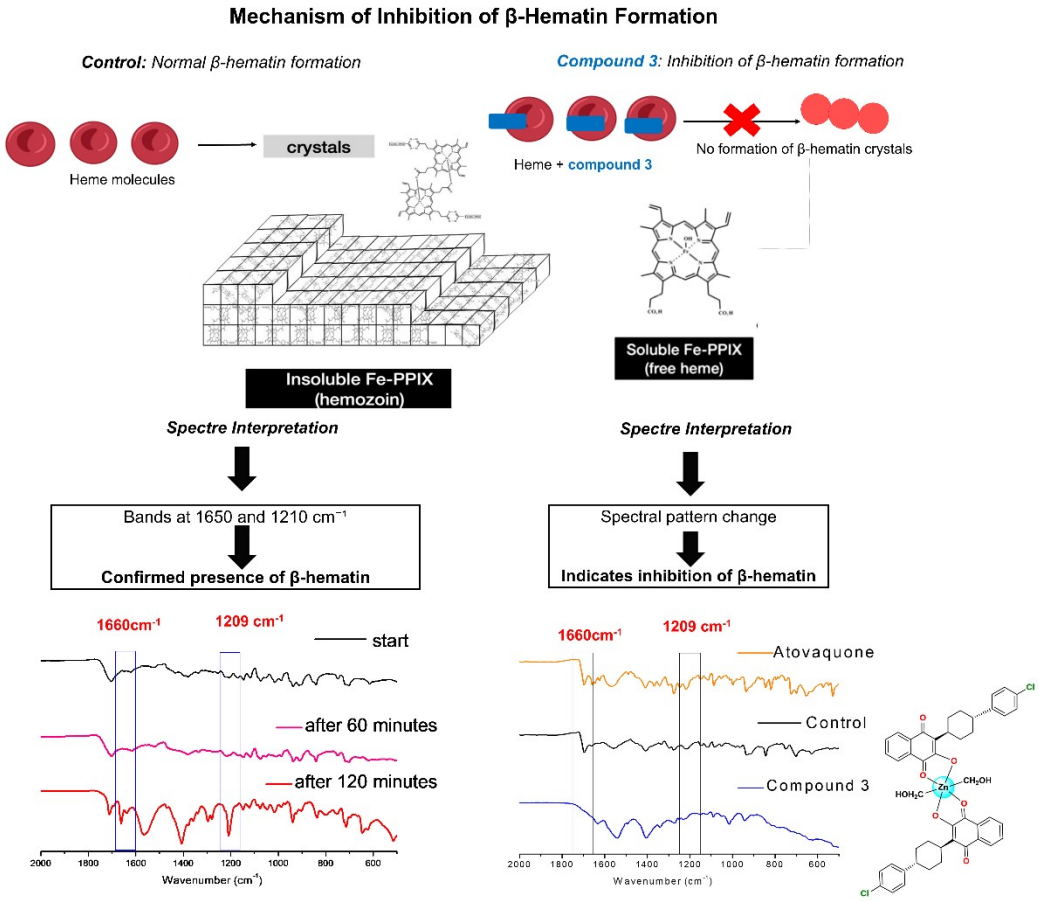

Figure S47: Inhibit β-hematin formation was further examined using FTIR spectroscopy (compound **3**)

Reference

[1] O. V. Dolomanov, L. J. Bourhis, R. J. Gildea, J. A. K. Howard and H. Puschmann, J. Appl. Cryst., 2009, **42**, 339–341.

[2] G. M. Sheldrick, Acta Cryst. A, 2015, **71**, 3-8.

[3] M. J. Frisch, G. W. Trucks, H. B. Schlegel, G. E. Scuseria, M. A. Robb, J. R. Cheeseman, G. Scalmani, V. Barone, B. Mennucci, G. A. Petersson, H. Nakatsuji, M. Caricato, X. Li, H. P. Hratchian, A. F. Izmaylov, J. Bloino, G. Zheng, J. L. Sonnenberg, M. Hada, M. Ehara, K. Toyota, R. Fukuda, J. Hasegawa, M. Ishida, T. Nakajima, Y. Honda, O. Kitao, H. Nakai, T. Vreven, J. A. Montgomery, J. E. Peralta, F. Ogliaro, M. Bearpark, J. J. Heyd, E. Brothers, K. N. Kudin, V. N. Staroverov, R. Kobayashi, J. Normand, K. Raghavachari, A. Rendell, J. C. Burant, S. S. Iyengar, J. Tomasi, M. Cossi, N. Rega, J. M. Millam, M. Klene, J. E. Knox, J. B. Cross, V. Bakken, C. Adamo, J. Jaramillo, R. Gomperts, R. E. Stratmann, O. Yazyev, A. J. Austin, R. Cammi, C. Pomelli, J. W. Ochterski, R. L. Martin, K. Morokuma, V. G. Zakrzewski, P. Voth, J. J. Salvador, S. Dannenberg, A. D. Dapprich, Ö. Daniels, J. B. Farkas, J. V. Foresman, G. A. Cioslowski and D. J. Fox, Gaussian 09, Revision D.01, Gaussian, Inc., Wallingford, CT, 2009.

[4] T. T. Adejumo, N. V. Tzouras, L. P. Zorba, D. Radanović, A. Pevec, S. Grubišić, D. Mitić, K. K. Anđelković, G. C. Vougioukalakis, B. Čobeljić and I. Turel, Molecules, 2020, **25**, 4043.

[5] Z. Akbari, J. Mol. Struct., 2024, 1301, 137400

[6] T. T. Adejumo, N. V. Tzouras, L. P. Zorba, D. Radanović, A. Pevec, S. Grubišić, D. Mitić, K. K. Anđelković, G. C. Vougioukalakis and B. Čobeljić, Molecules, 2020, 25, 4043.